THE DETERMINATION OF THE RELATIONSHIP BETWEEN TRANSPIRATION RATE AND DECLINING AVAILABLE WATER FOR *EUCALYPTUS GRANDIS*

by

PJ DYE, AG POULTER, S SOKO AND D MAPHANGA

Division of Water, Environment and Forestry Technology

CSIR

Nelspruit

WRC Report No : 441/1/97
ISBN No : 1 86845 305 7

EXECUTIVE SUMMARY

Transpiration from South African forest plantations is believed to account for a large fraction of the total rainfall falling in afforested catchments (Dye, 1993). A model of potential transpiration rates from different age classes of *Eucalyptus grandis* (the most widely planted hardwood species) has recently been developed from plantations in relatively high rainfall areas east of Sabie (Olbrich, 1994). This species is frequently grown in areas receiving relatively low rainfall where the trees experience periodic, significant soil water deficits. The use of potential transpiration models to simulate transpiration rates in such areas will lead to overestimates of water use when soil water deficits limit transpiration rates.

The aim of this study was to determine the relationship between soil water availability and transpiration rates by plantation *E. grandis*, and to assess the feasibility of modelling the soil water balance in order to estimate the degree of reduction in transpiration under conditions of sub-optimal soil water supply. Some of the more specific questions relating to the practicality of the approach were as follows:

- What is the maximum rooting depth, and how does it vary with tree age?
- Is soil water abstracted and recharged uniformly?
- Does the moderating function change as the trees grow older?
- Is this function altered by seasonal changes and site differences?
- Do potential transpiration models apply to all stands with sufficient soil water

availability?

- What is the progression of physiological response to soil water stress, and how is transpiration rate reduced?
- How fast does the transpiration rate recover after water stress is relieved?

Three different sites were selected for investigation. At each site, plastic sheeting was laid over the ground to prevent soil water recharge and thereby allow the tree roots in the soil to induce a continuous progressive depletion of soil water. Initial work took place at two experimental sites in Frankfort Plantation in the Sabie area of Mpumalanga. Site 1 supported a stand of three-year-old *E. grandis* trees, while nine-year-old trees were growing on site 2, situated 2 km away. At site 1. measurements of pre-dawn xylem pressure potential (XPP), leaf area index (LAI), stomatal conductance, growth and sap flow rates took place from June 1992 to June 1993, while measurements of pre-dawn XPP, LAI, growth and sap flow at site 2 lasted from June 1992 to January 1993. At both sites, prevention of soil water recharge resulted in only relatively low levels of stress developing in the trees. Neutron probe readings at site 1 showed the trees to be vigorously abstracting water down to the deepest measurement depth (8 m below the surface). Similarly, at site 2, the trees were found to be obtaining much of their water requirement from depths below 8 m. Neutron probe readings at the start and end of the treatment periods were converted to volumetric soil water contents to determine the total water abstraction over these periods. The calculations showed that only 46 % of the recorded sap flow in the sample trees came from the 8 m profile at site 1, and only 37 % at site 2. The conclusion at both sites was that the relation between

transpiration and soil water availability could not be defined, since the rooting zone extended well below the deepest measurement depth, and that the trees displayed only early signs of stress in consequence of their ability to obtain significant quantities of water below 8 m. Modelling the soil water balance of such deep profiles is considered to be impractical, especially on the scale of whole catchments, in view of the problem of measuring soil water content at depth, the heterogeneity of deep subsoil material, the unknown volume of stones, and the likely non-uniform infiltration of water through the deeper strata.

With the above conclusion in mind, a third site was chosen in an area with a lower mean annual rainfall (950 mm) and with a shallower soil profile (18 m). This site was situated on the HL&H estate of Legogote North East in the vicinity of White River. Measurements of sap flow, trunk growth, xylem pressure potential, leaf area index, stomatal conductance, and soil water contents took place between February 1994 and December 1995. In contrast to the Frankfort results, the trees experienced substantial late-winter stress in 1994 due to soil water deficits. This was prior to the plastic sheeting being laid out in April 1995. This stress was sufficiently high to cause a marked decline in leaf area index, and reduced water use by the trees. Partial recovery took place during the following summer. Soil water abstraction amounted to 48 % of measured sap flow in the seven months the soil surface was covered by plastic sheeting. In contrast to the Frankfort sites, the deeper strata contained very little available water, and some evidence for a limited amount of lateral flux of water from the edge of the plot was recorded.

Comparison of sap flows, leaf area index and stomatal conductance between the Frankfort sites and the Legogote site led to the realization that potential transpiration models developed from trees in sites with high rainfall and deep soils will overestimate water use of trees in such drier sites, even during the summer months when soil water availability is high. I hypothesize that the site 3 trees experience regular stress during each winter which has led to adaptions involving lower leaf stomatal conductances, sapwood moisture content and leaf area indices, all of which serve to reduce the water use of the trees. This is a further complication to the original goal of moderating potential transpiration models on the basis of soil water contents to predict tree water use under water limited conditions.

The foregoing has led the author to believe that the only practical alternative to estimating the water use of eucalypt plantations on sites with limited water availability is to use the growth of the trees as an index of the water use. This project inspired a separate study of the correlation between *E. grandis* growth and water use. Data from 17 six-year-old trees from a wide range of sites in the White River area have shown a remarkably good correlation between annual volume growth increment and total yearly sap flow (Figure 1). The annual growth and water use data from the sites in this study conform to the trend. The implication of this good correlation is that maps of volume growth increments can be obtained for even the most heterogeneous catchments and used to estimate the annual water use of the trees. The growth/water use relation would obviously need to be verified for a

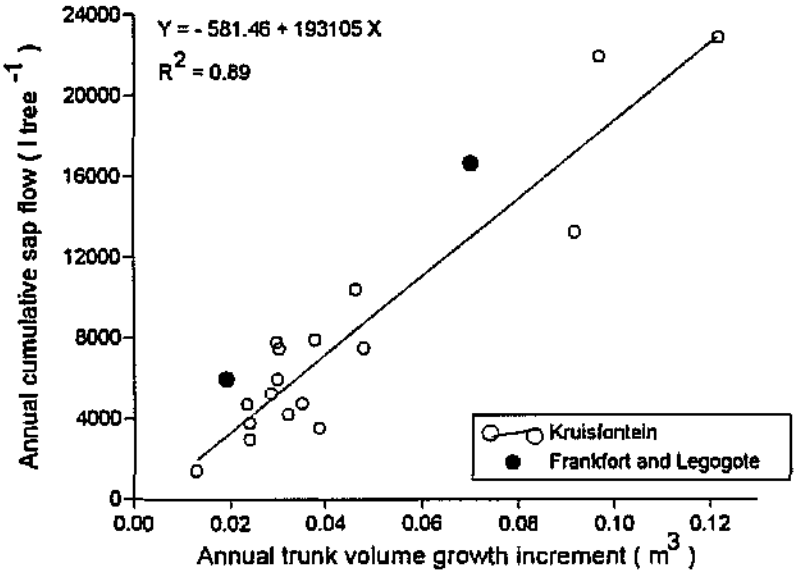

Figure 1. *The relation between yearly volume growth increment and yearly total sap flow recorded in 17 sample trees at Kruisfontein. The mean volume growth and total sap flow recorded at sites 1 and 3 are also shown.*

representative range of tree ages, site qualities, climates and genotypes. This verification has already commenced.

In conclusion, the aim of this study was to determine the feasibility of deriving and using a moderating function to simulate reductions in transpiration during times of significant soil water deficit. Results have demonstrated that this approach is impractical. However, they have provided many valuable insights into the relation between trees and soil water, and have led to an alternative strategy for estimating

water use by trees subject to a highly variable soil water supply. It is anticipated that the data collected during this study will be of great use in verifying models such as ACRU, and perhaps indicating where modifications are required.

KEYWORDS: *Eucalyptus grandis*, sap flow, transpiration, drought stress, soil water abstraction, water use efficiency

TABLE OF CONTENTS

LIST OF FIGURES

LIST OF TABLES

1. INTRODUCTION

A large proportion of the surface water resources of South Africa emanates from relatively small but important catchment areas concentrated along east- and south-facing escarpments and mountain slopes. These catchments were originally largely montane grassland, but today most have been converted to forest plantations, chiefly pines and eucalypts. The forestry industry is subject to ongoing criticism of the alleged excessively high water use of forest plantations, and is currently funding research to obtain clarity on this issue. As part of this initiative, the Division of Water, Environment and Forestry Technology, CSIR, is developing models to simulate transpiration rates of the major plantation species. Models to predict potential transpiration by well-watered *Eucalyptus grandis* Hill ex Maiden trees have been developed for five different age classes of trees (Olbrich, 1994). However, where eucalypt plantations suffer significant soil water deficits, transpiration rates will be overestimated by these models. One approach to simulating below-potential transpiration rates is to determine the relationship between transpiration rate and available soil water within the rooting zone. Modelling the water balance in the soil profile can then permit the prediction of what fraction of potential transpiration is taking place at a given time. Such moderating functions have been described before for eucalypts (Dunin and Aston, 1984; Calder, 1992), but their applicability to *E. grandis* growing on South African forestry sites is unknown.

2. AIM

The purpose of this study was to determine the relationship between soil water availability and transpiration rates by plantation *E. grandis*, and to assess the feasibility of modelling the soil water balance to estimate the degree of reduction in transpiration under conditions of sub-optimal soil water supply.

3. MATERIALS AND METHODS

3.1 Site descriptions and treatments

The relation between tree water use and soil water content was investigated on three different sites. At each site, approximately 900 m^2 of plastic sheeting was laid out around four sample trees, in order to prevent soil water recharge and induce a progressive drying of the soil by the tree roots. All sites were located on relatively flat ridge tops to minimize the possibility of lateral flow of water into or out of the sites. Two of the sites were chosen in Frankfort Plantation (24° 49′ S, 30° 43′ E) in the vicinity of Sabie, Mpumalanga. The plastic sheeting at both these sites was laid out in June 1992.

The Frankfort site 1 (compartment A19) supported an unthinned stand of three-year-old *E. grandis* trees planted at an espacement of 3.5 by 3.5 m (816 trees per hectare). The average ground area per tree in the immediate vicinity of this site was

13.5 m^2. The Frankfort site 2 (compartment A12a) supported a thinned stand of nine-year-old *E. grandis* trees at a density of 300 trees per hectare. The average ground area per tree at this site was 31.8 m^2. The two Frankfort sites were situated 2 km apart. The soils at both sites are deep rhodic ferrasols (FAO, 1974) derived from coarse-grained biotite granite of the Nelspruit Group. Deep drilling showed the permeable subsoil to extend beyond 30 m at each site. These soils have been associated with a forestry land classification system termed *Escarpment Foothills* (Louw, 1993) and calculated to comprise 29% of the approximately 590 000 ha of plantation forestry land in the province of Mpumalanga. Their silvicultural rating is listed as optimal, indicating prime growing conditions and therefore a greater importance than their area implies. The 20-year mean annual rainfall recorded in Frankfort State Forest is 1459 mm. Rainfall in the 10 years prior to the commencement of this experiment comprised 85% of this mean. At site 1, the plastic sheeting was left in place for 13 months, while at site 2, it was removed on 15 January, after a period of seven months.

A third site (site 3) was situated in compartment 39 on the property Legogote Northeast, owned by the forestry company HL&H. This site is 12 km north of White River (25° 13′ S, 31° 02′ E), at an altitude of 1050 m. The mean annual rainfall at the site is approximately 950 mm. The trees belonged to an FSC clone of *E. Grandis*, and were planted in December 1989. Initial planting espacement was 3 by 2.5 m, while the average ground area per tree close to the site was 13.1 m^2. Deep drilling revealed granitic bedrock to be at a depth of 18 m below the surface. Plastic sheeting was laid out on 19 April 1995, and remained in place until the experiment

was terminated in December 1995.

3.2 Weather records

A scaffolding tower was erected near the centre of site 1. The height was periodically increased to maintain it at approximately 1 m above the tallest adjacent tree. An automatic weather station was mounted on the highest frame. Sensors recorded temperature, relative humidity, photosynthetically active radiation, wind speed, wind direction and rainfall. Five minute rainfall totals were recorded by a tipping bucket rain gauge. All other sensors were programmed to record hourly means of one minute instantaneous measurements. No weather data were collected from site 2, due to the greater height of the trees and the proximity of this site to the site 1 weather station. A tower was erected close to the centre of site 3, and the identical weather station installed at the top.

3.3 Sap flow measurement

The heat pulse velocity (HPV) technique was used to monitor hourly sap flow rates in four adjacent sample trees at the centre of each site. Four probe sets per tree were implanted at site 1, where thermistors were positioned to depths of 5, 13, 23 and 35 mm below the cambium. These depths were chosen to place thermistors within the sapwood (determined through staining cross-sections of trees of similar size with methyl orange), and to be 5 mm from the sapwood/cambium and sapwood/heartwood interface. Probes were repositioned in January 1993 to adjust

for the diameter growth of the trunks. Eight probe sets per tree were implanted at site 2, two each at depths of 5, 11, 19 and 27 mm beneath the cambium. Four probe sets per tree were implanted into the four sample trees at site 3, to depths of 5, 13, 23 and 35 mm beneath the cambium. Three vertically aligned holes were drilled radially into the sapwood at each measurement position, using a 1.85 mm drill bit. A jig with a thickness of 20 mm was used during the drilling procedure to ensure that the drilled holes were parallel to each other. A line heater was inserted into the central hole, while temperature-sensing probes were implanted 10 mm above and 5 mm below the heater. The line heater consisted of a steel tube with an outside diameter of 1.8 mm. Temperature probes consisted of a single thermistor sealed within a Teflon tube of similar diameter. Each sensor probe thus gave a point estimate of sapwood temperature. Each thermistor pair was connected in a Wheatstone bridge configuration and automatically adjusted to zero output before each heat pulse initiation. The logger was programmed to apply a current of 30 Amperes lasting 0.5 s to each of the heaters. Heat pulse velocity was measured for each probe set using the compensation technique (Huber and Schmidt, 1937; Swanson, 1974). At the conclusion of each experiment, trunk segments containing the drilled holes were removed to measure precise probe separation distances at the original thermistor insertion depth. These distances were measured to the nearest 0.1 mm. Heat pulse velocities were corrected for sapwood wounding caused during the drilling procedure. Swanson and Whitfield's (1981) wound correction coefficients were used to derive corrected heat pulse velocities using correction coefficients appropriate to the measured wound size, diameter of Teflon probes, and probe separation distances. The size of the wound at each probe set location was

measured at the end of the experiment. These were of very similar magnitude to wound widths recorded in separate short-term HPV studies in the Sabie/White River area, implying that wound widths were stable over the experimental periods. The four or eight sections of the tree trunk containing the probe implantation holes were excised. Each block was re-cut longitudinally at the particular depth below the cambium where the thermistor was originally positioned. The exposed, fresh face was shaved smooth using a microtome, after which the darker wound tissue was identified. Wound width was measured to the nearest 0.1 mm using a 7X scale loupe. These measurements were taken midway between the line heater position and both the upper and lower thermistors. The corrected heat pulse velocities were converted to sapwood-specific sap flow (v) using the following equation (Marshall, 1958):

$$v = \rho_b(m_c + c_{dw})u \quad (1)$$

where ρ_b = dry wood density, m_c = moisture fraction of sapwood, c_{dw} = specific heat of dry wood, assumed constant at 0.33 (Dunlap, 1912), and u is the wound-corrected HPV. Wood density was calculated as dry weight per volume of a freshly excised section of sapwood. Volume was determined in the field by immersing the fresh wood sample in water and applying Archimedes' principle. Moisture fraction was calculated as (fresh weight - dry weight)/dry weight. The moisture fraction was assumed to be constant over the experimental period.

Marked radial differences in sap flow in *E. grandis* are the norm (Olbrich, 1994). Sap flow recorded at each probe depth was considered to be representative of a ring of

sapwood with limits defined by the midpoint between successive probe depths or by the interface with cambium or heartwood. Total sap flow was calculated as the sum of these partial areas multiplied by their associated sap flows. HPV estimates of sap flow in *E. grandis* have been compared to cut-tree uptake rates and shown to be accurate (Olbrich, 1991).

Measurements of sap flow at site 1 were recorded at hourly intervals from June 1992 to June 1993, and at site 2 from September 1992 to June 1993. Measurements at site 3 lasted from February 1994 to December 1995. Tree densities in the immediate vicinity of each site were recorded to permit conversion of sap flows per tree to mm equivalent depth of water.

3.4 Xylem pressure potential

A Scholander pressure chamber (Ritchie and Hinckley, 1975) was employed to make regular measurements of pre-dawn xylem pressure potential (XPP). At site 1, a sample leaf was taken at mid-canopy position from each of five trees within reach of the centrally located scaffolding tower. Another scaffolding tower positioned 50 m away from the study site was used to obtain sample leaves from four trees growing in soil subject to normal soil water recharge. A catapult was used to knock down leaves from 4-5 trees growing at the centre of site 2. No two leaves came from the same tree on a given date. At site 3, one sample leaf was taken at mid-canopy position from each of four trees within reach of the centrally located scaffolding tower. Both pre-dawn and mid-day readings were taken at this site.

3.5 Leaf area index

A Licor LAI-2000 plant canopy analyser (LI-COR, P.O. Box 4425, Lincoln, Nebraska, USA) was used to measure the nominal leaf area index (LAI) at regular intervals over the study periods. Readings were timed as far as possible to coincide with cloudy weather, or with low light conditions at dawn or dusk, to minimize reflectance of sunlight off the foliage. Measurements involved an initial above-canopy reading, followed by 10 below-canopy readings, and were concluded by a further above-canopy reading. The above-canopy readings at site 1 were taken from the top of the scaffolding tower, while at site 2 and 3 they were taken in clearings a short distance from the sites. The below-canopy readings were taken with the sensor positioned directly above each of the 10 access tubes. The resultant data files were modified using the LI-COR C2000 software to remove the data sensed by the two outermost rings (53 and 68° from the vertical) , before recalculating LAI. This procedure ensured that the LAI calculation was based on the canopy characteristics of trees close to the centre of the study sites.

3.6 Leaf stomatal conductance

Mid-day leaf stomatal conductances were recorded at sites 1 and 3. At site 1, ten sample leaves were labelled in the upper half of the canopies of five trees accessible from the tower. All leaves were fully expanded, disease-free and fully

exposed to the sun. Readings took place from 13h00 to 14h00. A LI-COR LI-1600 porometer (LI-COR, P.O. Box 4425, Lincoln, Nebraska, USA) with an aperture of 4 cm^2 was used at this site. At site 3, an MCS 301 null balance porometer (Mike Cotton Systems, P.O. Box 73, Steenberg, 7947, South Africa) was employed to record stomatal conductances on three sample leaves in each of four trees accessible from the tower. Readings were displayed or initially calculated in units of either resistance (s cm^{-1}) or conductance (cm s^{-1}), and converted to molar units using the following formula (Pearcy, *et al.*, 1989):

$$g_w \text{ (mol } m^{-2} s^{-1}) = g_w \text{ (cm } s^{-1}) * 0.446 * (273 / (T+273)) * (P / 101.3) \quad \textbf{(2)}$$

where T = temperature (°C) and P = atmospheric pressure (kPa).

3.7 Trunk growth

The growth of the trunks of the four sample trees was monitored at regular intervals throughout the experiment at sites 1 and 3. Measurements of diameter growth were insufficiently sensitive at site 2 to show an increase in girth over the experimental period. At site 1, simultaneous diameter and height measurements were also made on four trees situated a short distance away from the experimental site, where soil water recharge was unhindered. On each sample day, tree heights, as well as the diameters at 1.3 and 5 m above the ground were carefully measured. Tree heights were recorded by raising height rods adjacent to each sample tree until an observer

at the top of the tower judged the top of the rod to be at the level of the highest leaf. Trunk volumes were calculated as follows. The portion of the trunk from ground level to 1.3 m was assumed to be a cylinder with a diameter equal to that recorded at 1.3 m. The volumes of the segment between 1.3 and 5 m was calculated assuming it to be a frustum of a cone. The last segment between 5 m and the top of the tree was assumed to be a cone.

At site 3, only DBH and height were recorded. Trunk volumes were calculated using the Demaerschalk model as described by Coetzee (1992).

3.8 Soil water measurement

At each site, a pneumatic crawler rig was used to install 10 aluminium access tubes (with a diameter of 51 mm) to a depth of 8.5 m. These were arranged in an area of approximately 10 by 10 m centred on the four sample trees at each site. Figure 2 illustrates the arrangement of the holes in relation to the trees at site 1, showing how they were positioned at varying distances from the trees. A CPN 503 hydroprobe (Campbell Pacific Nuclear Corporation, 130 South Buchanan Circle, Pacheco, California, 94553, USA) was used to take regular readings of neutron counts (60 s recording periods) at depths of 0.25, 0.5, 0.75, 1, 1.25, 1.5, 1.75, 2, 3, 4, 5, 6, 7 and 8 m below the surface. Counts were expressed as a ratio of soil count to standard count measurement recorded in the field just prior to the start of

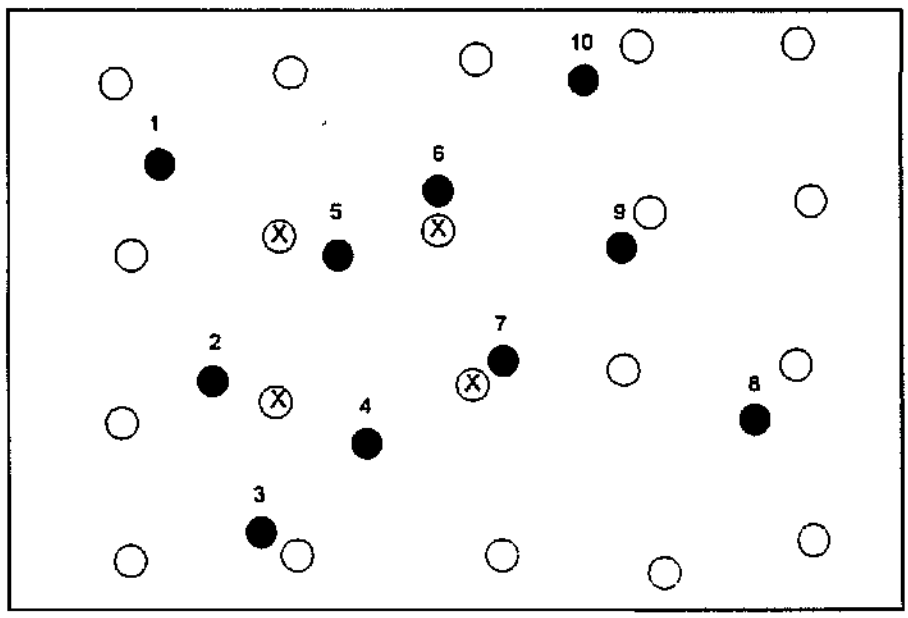

Figure 2. *A map of the positions of access tubes (solid symbols) and trees (open symbols) at site 1. Access tubes are identified by numbers, while the four sample trees are identified by an X.*

measurements. These standard counts were recorded with the neutron probe source locked in position in the shield, and mounted on a reference access tube. Regarding the calibration of neutron probe data, it was considered impractical to follow the standard drum calibration methods (as described by Greacen, 1981) for the deep profiles in this study. Potential problems with this technique were perceived to be the difficulty of obtaining sufficient quantities of soil from the deeper levels, as well as the problem of recreating the original bulk density within the drum. A field calibration procedure was attempted but found to be impractical, since moisture changes over time, particularly in the deeper strata, were too small to define the slope of the calibration relation. It was therefore decided to make use of a soil calibration service offered by the French Cadarache Nuclear Research Centre.

The method is based on the use of a mathematical model of neutron scattering in soil around a fast neutron emitter to calculate the thermal flux of neutrons from measured values of the thermal absorption ($\sum a$) and diffusion ($\sum d$) cross-sections of the soil. These values are determined in a graphite pile of 1 m^3 containing a source of three curies of Am/Be at its centre. A thermal neutron detector measures the perturbation introduced by a 300 g sample of disturbed soil placed in the pile between the source and the detector. The ratio of count rates obtained with and without the soil sample in the pile is a function of the thermal cross-section ($\sum a$). A second detector placed at the outside of the graphite block measures the thermal neutrons transmitted through the soil sample. Its relative count rate is related to the diffusion constant ($\sum d$). The calibration curve of a soil has the form:

$$N=(\alpha\rho + \beta)\theta + \gamma\rho + \delta \qquad (3)$$

where α, β, γ, and δ are physical constants of the soil, determined from the measurements of $\sum a$ and $\sum d$, ρ is the dry density (g cm^{-3}), θ is the percentage volumetric water content, and N is a normalized count rate, equal to the count rate which would be obtained with a probe producing 1000 cps in water (Couchat *et al.*, 1995). Calibrations using this technique have been compared with gravimetric field calibrations for several soils in Europe, and found to compare very favourably (Vachaud *et al.*, 1977).

A modified form of equation 3 was used in which the neutron probe counts are expressed relative to counts recorded with the source in water. Counts in water

were recorded by immersing a 2 m length of access tube into a small dam, in a position where the neutron probe source was surrounded by 90 cm of water in every direction. The lower end of the access tube was sealed to prevent entry of water. The mean count rate over 40 1 minute counts (29767), as well as mean standard count (10825) over 14 1 minute counts (with the source within the housing), were recorded. Count ratios based on standard counts recorded with the source locked in the shield were converted to ratios based on standard counts in water. This was achieved by dividing the standard count recorded in the field by 10825 and multiplying by 29767.

Equation 3 includes soil bulk density. This was measured at each neutron probe measurement depth. An auger with a standard 10 cm bucket was used to reach each sample depth. A bulk density sampler was then carefully pushed into the undisturbed soil and then withdrawn to the surface. The sample cup was withdrawn from the sampler, and excess soil removed from either end of the cup before plastic lids were fitted to either end of the cup. These cups were oven-dried at 105 °C and then weighed. Bulk density was calculated as the dry mass of the soil (minus the weight of the cup) divided by the volume of the cup. On the basis of soil bulk density data at each site, it was decided to obtain neutron probe calibrations for the soil at depths of 25, 100 and 300 cm below the surface. Soil samples from these depths were retrieved from three cores per site, and thoroughly mixed together before being submitted to the Cadarache Nuclear Research Centre.

3.9 Lateral and vertical soil water influx

3.9.1 General methodology

The placement of the plastic sheeting around the sample trees at each site caused soil water contents to decline as further recharge of soil water from the surface was prevented. Changes in soil water content at a particular depth can be assumed to comprise the entire quantity of water abstracted by the roots at that depth. However, this assumption may be erroneous if significant gradients in soil water potential developed within the monitored volume of soil, leading to significant inward movement of water from the edge of the plastic sheeting, or upward movement from deeper strata. The true net water use by trees at each level is equivalent to the change in soil water storage within the representative volume at that level **plus** the vertical and horizontal fluxes of water into the monitored volume of soil. The observed water contents at each level were translated into matric pressure heads by means of representative water retention characteristics for the level. Hydraulic gradients were then determined for the time intervals between observations and hence soil water fluxes into the representative volume elements were calculated for each period. The hydraulic conductivity used to calculate these fluxes was determined from the conductivity characteristic derived from *in-situ* infiltrometer measurements.

The homogeneity of the soils was investigated by assessing the variability of the textural and bulk density measurements at different depths for each profile. Typical

water retention characteristics for the different levels were then determined from undisturbed samples. Hydraulic characteristics were estimated in-situ to a depth of only 1.5-1.7m. Hence, hydraulic conductivity characteristics at depths deeper than this had to be deduced from relationships between the physical properties, the water retention characteristics and the hydraulic conductivity relationships. These relationships were determined and verified at the levels where all three of these soil characteristics were measured.

3.9.2. Measurement of soil physical and hydraulic properties

Soil testing was performed both in-situ and in the laboratory. The samples for laboratory analyses were taken from positions immediately adjacent to where in-situ testing took place. In addition, undisturbed samples from soil cored to a depth of 5 m were tested in the laboratory for textural, bulk density and water retention analyses. The following procedures and analyses were performed:

- An *in situ* tension infiltrometer test was performed with a minimum of 3 tensions to produce the unsaturated hydraulic conductivity of the wet end of the characteristic.

- An *in situ* double ring ponded infiltration test was performed on the same position as the tension infiltrometer test to yield the saturated hydraulic conductivity.

- A 10 cm diameter x 8 cm deep sample was extracted from the position of the tension infiltrometer using a thin walled sampler.

- Sub-samples of 5.5 cm diameter and 3 cm deep were cored from the 10 cm diameter sample.

- These sub-samples were also used to determine the bulk density of the material.

- The sub-samples were used to determine the water retention characteristic using a controlled outflow cell. An additional estimation of the hydraulic conductivity was made on some of the samples during the controlled outflow cell test.

- A particle size analysis was performed on three sets of augered core samples for each site. Both sieve and hydrometer tests were completed.

- The bulk density was determined using each of these augered samples. Porosities were calculated from the bulk density results.

Each of the methodologies is briefly described below.

Bulk density and porosity The bulk density was determined from the mass and volume data of the sub-sample rings. Care was taken at all times to ensure the

materials were not significantly disturbed. The porosity (ϕ) was calculated using the bulk density, ρ_b and the particle density, ρ_s as

$$\phi = 1 - \frac{\rho_b}{\rho_s} \tag{4}$$

Particle size distribution A hydrometer test was performed on approximately 100 g of sub-sample for a period of 36 hours. Determination of particle size and per cent finer was calculated using a particle density of 2.65 g cm^{-3}. On conclusion of the hydrometer test, the material was poured through a series of 7 sieves ranging in size from 0.053 to 2 mm opening. The material on each sieve was washed through to the next in a wet sieving process, ensuring that the hydrometer and sieve tests were performed on the same sub-sample material.

Measurement of hydraulic characteristics The hydraulic properties measured were the water retention characteristic and the hydraulic conductivity characteristic. The water retention characteristic was measured with a controlled outflow method, while the hydraulic conductivity characteristic was measured by in-situ ponded and tension infiltrometer tests as well as by a laboratory outflow cell method.

Water Retention Characteristic The controlled outflow cell method makes use of an outflow cell (figure 3) developed at Colorado State University (Lorentz, Durnford and Corey, 1991; Lorentz 1993) and modified for hydraulic conductivity

measurements at the University of Natal (Lorentz, 1994). Liquid is forced out of the sample by increasing the air pressure in the cell. The volume of outflow is regulated by closing the stopcock so that the retention characteristic is developed by controlling the water content rather than the matric potential as in most common methods. The equilibrium matric potential head is observed by monitoring the pore water pressure after the stopcock is closed. By judicious application of air pressure, the effects of hysteresis can be minimised and a very detailed retention characteristic can be developed, especially at the wet end of the characteristic. This is most useful when used in conjunction with tension infiltrometer tests to determine the effects of macropore flow and hydraulic conductivities in nearly saturated soils. All materials were tested to a matric pressure head of approximately 1000 cm (1 bar). Additional data points were measured for selected soil samples at a pressure of 3000 cm (3 bar) and 15000 cm (15 bar), using conventional pressure chamber equipment.

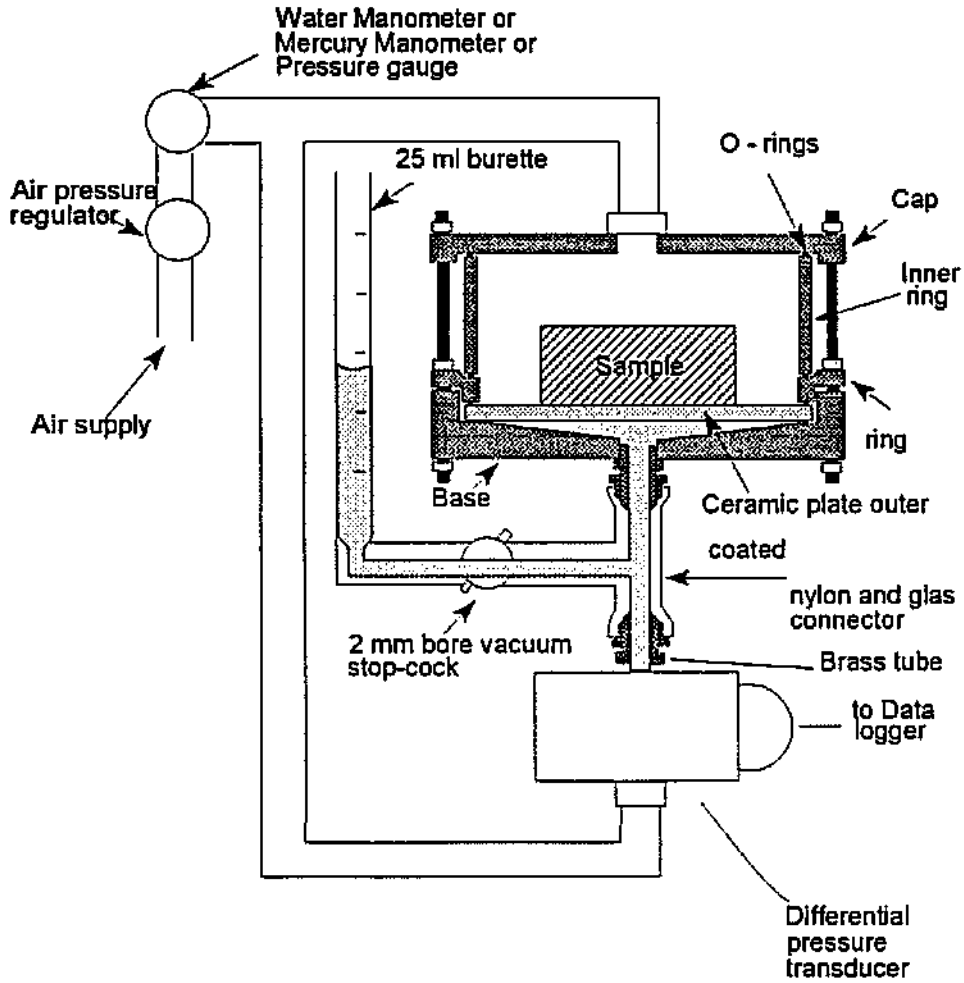

Figure 3. Schematic section of the controlled outflow cell.

Hydraulic conductivity characteristic The hydraulic conductivity characteristic was determined for all soil samples by in-situ tension and ponded infiltrometer tests. Additional hydraulic conductivity determinations were made at a range of matric pressure heads during the laboratory controlled outflow tests for

selected samples.

Regression constants were fitted to the steady state portion of the infiltration data. The double ring constants were used to estimate the hydraulic conductivity at saturation while the tension infiltrometer constants were used to determine the hydraulic conductivity at the matric pressure head applied during the test. The theoretical analysis proposed by Ankeny (1992) was used to calculate the hydraulic conductivities from the regression constants.

The controlled outflow cell was modified to determine hydraulic conductivities. A small ceramic plate with base and associated pressure transducer was constructed and placed on the top of the samples throughout the tests. During the outflow stage of each increment of the retention curve development, the matric pressure head was deduced from the transducer readings at the top and base of the sample. This permitted the hydraulic gradient across the sample to be estimated and, together with the recorded outflow rate, the hydraulic conductivity was calculated for the average matric pressure during the outflow period.

3.9.3 Development of typical hydraulic characteristics for each site

Before fluxes of water into the zone of interest could be calculated, a set of typical hydraulic characteristics needed to be developed for each site. These characteristics were then used to estimate the hydraulic gradients and the

associated hydraulic conductivity for the measured soil water contents in the access tubes. A methodology was developed to determine typical characteristics for each site by relating as much of the plentiful soil physical characteristics to the less frequently measured hydraulic characteristics. The following methodology was adopted:

3.9.3.1 Development of general water retention characteristics trends to 500 cm.

In order to develop a generalized water retention characteristic for each level at each site, use was made of empirical relationships proposed by Hutson (1984), but which were modified in this study to suit the observed soil properties. These relationships use the particle size distribution and bulk density data to represent the water retention data at various levels at each site. The measured particle size distribution and bulk density data were first used in an interpretation of textural trends to 500 cm. These typical data were then used in an initial regression equation of Hutson (1984) as described in Lorentz *et al.* (1996).The regression constants were subsequently varied in order to successfully represent the measured data for the water contents at 0.1 bar and 15 bar derived from water retention characteristics of selected samples from the surface to 500 cm. Once these regression constants were successfully estimated, general water retention characteristics could be developed for each horizon at each site. Selected points from these retention characteristics were extracted to show the variation in the characteristics with depth.

3.9.3.2 Simultaneous curve fit to water retention and hydraulic conductivity data

Pairs of theoretical curves which describe both the water retention as well as the hydraulic conductivity characteristics using a single set of parameters have been reported in the literature. The most versatile pair of these theoretical curves is that of Van Genuchten, details of which are provided by Lorentz *et al.* (1996). These curves were used to simultaneously describe the general water retention characteristic data together with the *in-situ* saturated and unsaturated hydraulic conductivity to a depth of 200 cm. These simultaneous fits could only be performed with data to 200 cm since this was the depth of the pits excavated for the measurement of the hydraulic conductivity. Once the theoretical curve parameters had been successfully determined over this depth, the generalised water retention data were used with associated theoretical curve parameters to extend the hydraulic conductivity theoretical curve data set to 500 cm. A further extrapolation of both the retention and hydraulic conductivity data was then performed to estimate these characteristics to a depth of 800 cm. General trends in the characteristics from 200 to 500 cm were used to perform this extrapolation.

3.9.4 Mass balance calculations

The water flowing inwards towards a representative volume of the profile is estimated by first determining the potential gradients towards elements of this volume in the lateral and vertical direction. The potentials are estimated from the

generalised water retention characteristics using the water contents measured in the neutron probe access tubes. The hydraulic conductivities at each level in each access tube were estimated from the characteristics developed above using the measured water content at that level. A logarithmic average hydraulic conductivity is determined to estimate the flux between two access tubes (for lateral flux estimations) or between two levels (for vertical flux estimations).

The development of potential gradients can be observed over time by comparing the differences in water contents at a particular level on a longitudinal profile between access tubes outside the representative volume and those closer to the centre of the covered area. Such comparisons were made for all three sites, at each soil level and for at least three longitudinal profiles, as well as in the vertical direction. The net volumes of water moving into the representative volume and not exiting were deemed to be utilized by the trees. It is important to emphasize that these flux estimates were made assuming homogeneous soil characteristics over the area of monitoring tubes. Typical soil hydraulic characteristics were assigned to each site and these characteristics were assumed to represent the horizons at every monitoring tube at that site. The spatial variability of certain soil physical characteristics were examined and appeared to be reasonably homogeneous. Hence the hydraulic characteristics, measured at only one profile, were taken to be a reasonable representation of the whole area and therefore the flux calculations were considered to be a reasonable estimate of the net soil water movement into the representative volume.

3.10 Soil depth

An attempt was made at each site to determine the depth to bedrock. At site 1, the pneumatic crawler rig was used to bore down to a depth of 38 m, at which point the air pressure became insufficient to blow the spoil back to the surface. At site 2, the maximum depth achieved was 31 m. At both these sites, no sign of bedrock was found. At site 3, bedrock was reached at a depth of 18 m.

An additional technique was employed at sites 1 and 2 to ascertain the depth to bedrock. Measurements of soil resistivity are widely used by geophysicists and exploration geologists to determine the characteristics of deep subsoils. The technique involves driving a series of steel pins (electrodes) into the ground at regular, equal intervals along a transect. In any group of four electrodes, the outer pair are current electrodes through which a known current is passed into the earth. The inner pair of electrodes are potential electrodes, between which a potential difference is measured. The penetration of the current increases as the distance between the current electrodes is increased. The effective depth of penetration is generally taken as approximately equal to the electrode separation. Thus repeated measurements of resistivity along the transect, and at different electrode separation distances, permits a two-dimensional picture of profile resistivity to be built up. Further details of this technique are described by Van Zijl (1985). Resistivity data were recorded at sites 1 and 2 along a 140 m transect, and to a depth of 40 m.

4. RESULTS

4.1 Frankfort site 1

4.1.1 Sap flow measurement

A summary of various tree characteristics relating to the calculation and interpretation of sap flow is shown in table 1.

Hourly sap flow rates were summed over the daylight hours each day to calculate the daily water use. The mean water use of all four sample trees at site 1 is shown in figure 4. Daily water use averaged approximately 30 litres per day during the 1992 winter, but rose markedly in spring in response to higher air temperatures and increased water vapour pressure deficits. Peak daily water use reached 90 litres per day (7 mm per day) on hot dry days in mid-summer. As expected, water use declined with the approach of the following winter, due to lower temperatures and shorter day length. There is no indication that sap flow declined during the study period as a result of increasing soil water deficits. The total sap flow of the four sample trees, from 1 June 1992 to 28 June 1993, was equivalent to 1325 mm. Mean daily sap flow over the entire year equalled 46 litres per tree.

Table 1. A summary of age, height, diameter at breast height (DBH), leaf area, sapwood moisture fraction, sapwood density and wound width of all four sample trees recorded at site 1 at the conclusion of the study in July 1993. Standard deviations appear in brackets. Mean leaf areas were estimated by stripping all leaves from the sample trees and estimating total area from total mass using the relation determined from a sub-sample of leaves.

	Frankfort site 1
Age (years)	4
Mean height (m)	14.7 (1.01)
Mean DBH (cm)	14.7 (1.17)
Mean leaf area per tree (m^2)	62 (11.82)
Mean sapwood moisture fraction	1.37 (0.162)
Mean wood density (g cm^{-3})	0.45 (0.040)
Mean wound width (mm)	2.83 (0.289)
Mean ground area per tree (m^2)	13.5

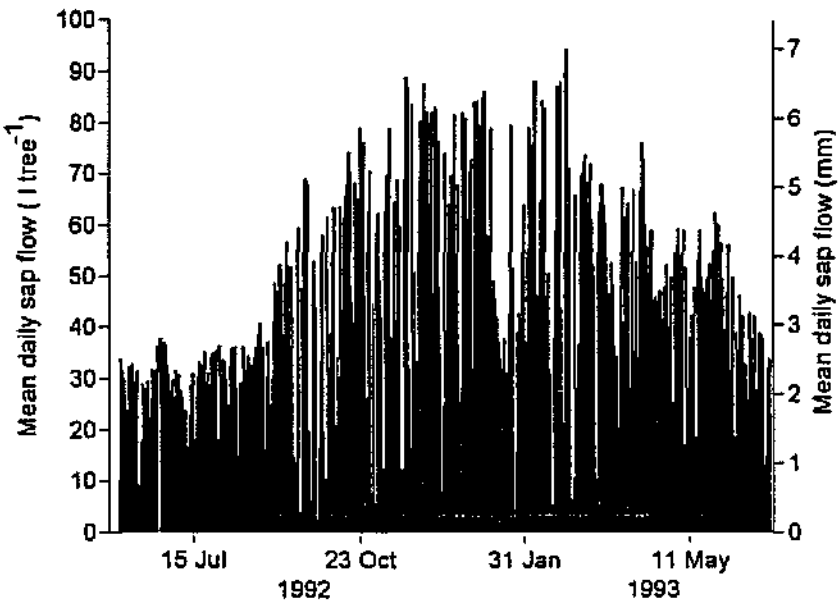

Figure 4. Total daily sap flow (mean of four trees) recorded at site 1.

4.1.2 Pre-dawn xylem pressure potential

Figure 5 shows the trend in pre-dawn XPP recorded at site 1. The trees under plastic appeared to exhibit a weak annual oscillation. Least negative potentials occurred in March-May, after which they become progressively more negative as the rainless winter progressed. This trend is even more distinct if the readings taken on 11 August and 6 October are omitted. On both these days, the canopy was wet due to prior rainfall, and field experience has shown that these conditions cause less negative XPP. This seasonal oscillation has been reported in an unrelated study (Dye and Olbrich, 1991). There was a clear difference in pre-dawn XPP between the

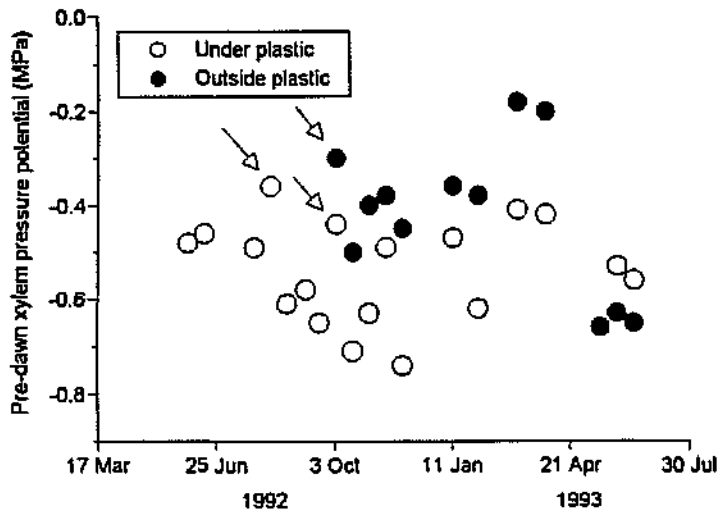

Figure 5. *Site 1. The trends in mean pre-dawn xylem pressure potential recorded in four sample trees under plastic sheeting, and four trees outside of the plastic sheeting experiencing normal soil water recharge. Arrows indicate days when the canopy was wet.*

trees under the plastic sheeting (open circles) and those outside (closed circles), showing that the former were experiencing somewhat more negative pre-dawn XPP due to the prevention of soil water recharge. This difference disappeared in May and June 1993 as the soils outside the plastic sheeting dried out.

4.1.3 Leaf area index

Figure 6 shows the trend in leaf area index at site 1. Little change in LAI was recorded over the study period, demonstrating that the trees were not reducing their

leaf area in response to soil drying.

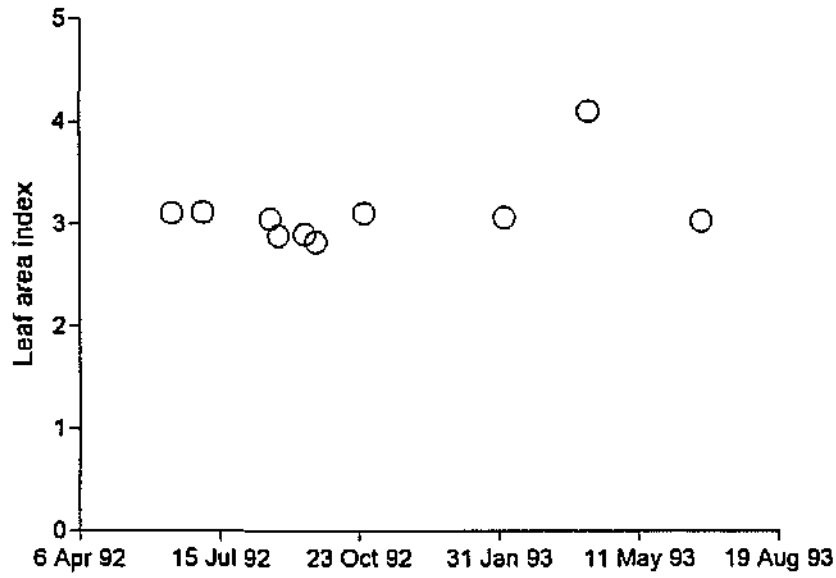

Figure 6. The trend in leaf area index recorded at site 1.

4.1.4 Leaf stomatal conductance

The mean leaf conductance trend (figure 7) lies mostly within the range of 200 to 400 m mol m^{-2} s^{-1}, but with a peak in late July and a larger peak in September. A spring-time increase has been observed before in this species (Dye and Olbrich, 1991), which cannot be explained from changes in ambient VPD. It is believed that a physiological change in the leaves may be responsible for this phenomenon.

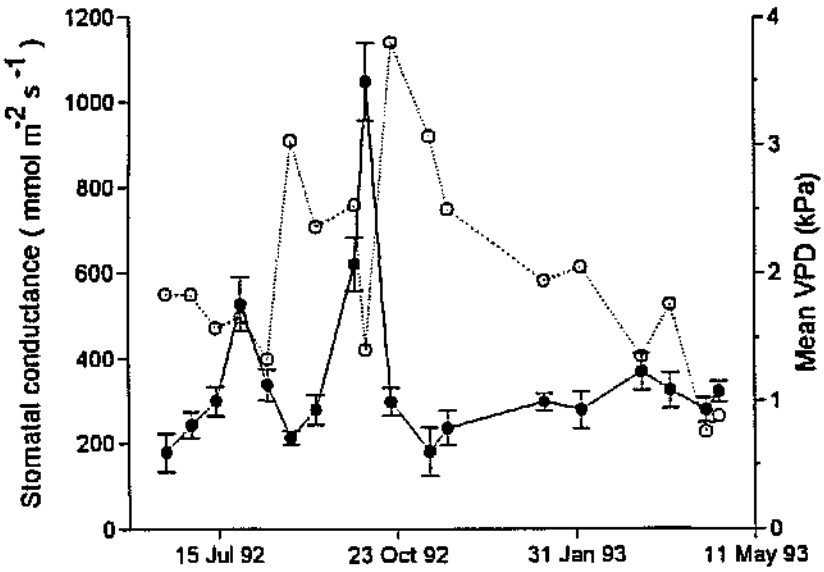

Figure 7. *The trend in stomatal conductance (mean of 10 leaves) recorded at 13h00 in upper canopy leaves exposed to sunlight at site 1. Bars indicate standard errors. Mean VPD is shown as open symbols.*

4.1.5 Trunk growth

Figure 8 shows the mean trend in DBH (diameter at breast height) and height for both groups of trees. Regarding DBH, the trees under plastic showed no reduction in rate of diameter growth over the monitoring period. The trees outside the area of plastic sheeting showed only a marginally higher growth rate. In contrast, a measurable difference in height growth between the two groups of trees took place in the second half of the experiment, with the trees under plastic showing

progressively slower growth rate. Both groups of trees showed a similar trend in height growth, which was fastest during the summer months and slower during the winter months. The data suggest that the influence of the treatment on the growth of the trees under plastic was relatively small.

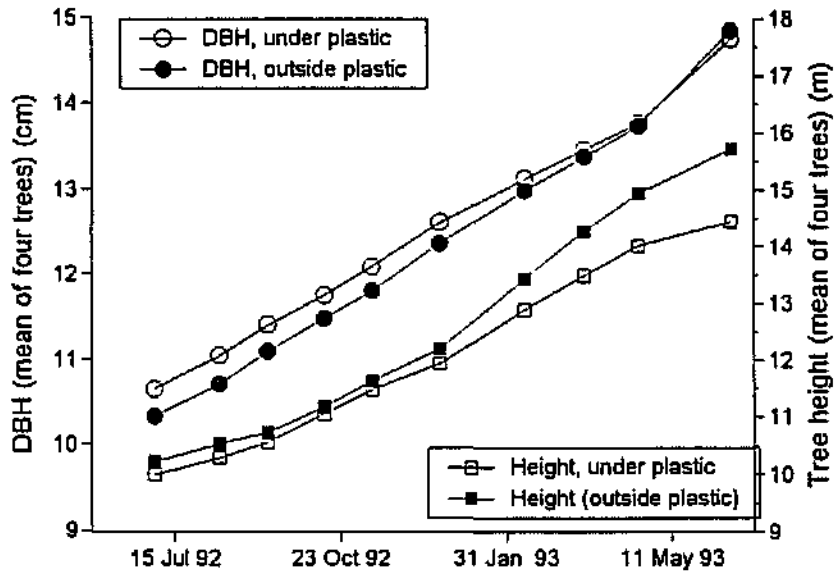

Figure 8. The trends in trunk volume and height increments recorded at site 1.

4.1.6 Apparent soil water abstraction

Table 2 shows the calibration equations pertaining to the three soil samples at site 1. It was assumed that the calibration equation determined for soil at 25 cm depth was applicable to 50 cm as well. Similarly, the 100 cm calibration was applied to 75, 125 and 150 cm, while the 300 cm calibration was applied to 175, 200, 400, 500,

600, 700 and 800 cm depths.

Table 2. Calibration equations pertaining to three soil horizons at site 1. R = counts at the sample depth; Rw = counts in a water standard.

Depth (cm)	Calibration equation
25	$\theta = 0.0847 * R/Rw - 0.0426$
100	$\theta = 0.845 * R/Rw - 0.0941$
300	$\theta = 0.918 * R/Rw - 0.0706$

Figures 9 and 10 show the pattern of soil water change as calculated from calibrated neutron probe readings. It is clear that significant soil water uptake took place, particularly at depths between 2 and 8 m. The data also suggest that abstraction became relatively greater at deeper levels after November 1992, presumably as available soil water in the upper strata became depleted. A sharp change in count ratio between 1 and 2 m is attributed to soil textural changes.

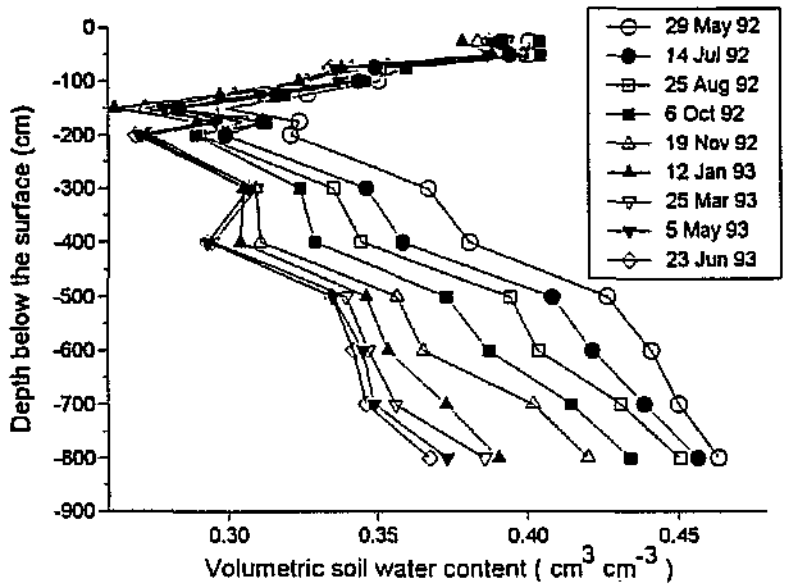

Figure 9. Changes in volumetric soil water content recorded in the soil beneath the sample trees at site 1.

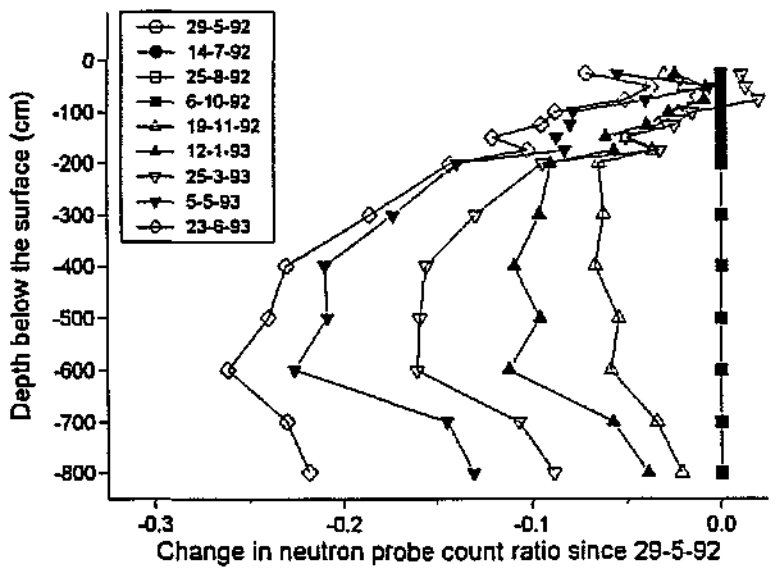

Figure 10. Changes in neutron probe count ratio (relative to readings recorded on 29 May 1992) recorded in the soil beneath the sample trees at site 1.

Table 3 summarizes apparent soil water uptake recorded at each measurement depth between 29 May 1992 and 23 June 1993. Sap flow over the same period measured 1325 mm. If the assumption is made that gradients in soil water potential led to negligible inflow or outflow from the monitored soil volume, then the trees obtained only 46% of their water requirement from the first 8 m of soil.

Table 3. The apparent soil water uptake recorded at each measurement depth between 29 May 1992 and 23 June 1993 (390 days). Total uptake is compared to sap flow over the same period.

Depth (cm)	Soil water (cm^3 cm^{-3}) (29-5-92)	Soil water (cm^3 cm^{-3}) (23-6-93)	Difference (cm^3 cm^{-3})	Horizon depth (mm)	Soil water uptake (mm)
25	0.401	0.387	0.013	375	5
50	0.400	0.385	0.015	250	4
75	0.354	0.334	0.019	250	5
100	0.35	0.338	0.013	250	3
125	0.327	0.308	0.018	250	5
150	0.299	0.279	0.020	250	5
175	0.324	0.294	0.030	250	8
200	0.321	0.269	0.052	625	33
300	0.367	0.307	0.060	1000	60
400	0.381	0.293	0.088	1000	88
500	0.426	0.335	0.092	1000	92
600	0.441	0.342	0.099	1000	99
700	0.45	0.346	0.104	1000	104
800	0.463	0.367	0.096	1000	96
Total					607
			Total sap flow (mm)		1325
			% of total sap flow		46%

4.1.7 Lateral and vertical soil water influx

Table 4 summarizes the set of *in-situ* and laboratory measurements recorded at this site.

Table 4. A summary of soil physical and hydraulic property tests performed at site 1, Frankfort Plantation.

Depth	Texture and bulk density				Water retention				H.C.
	Pit	Core samples			Pit	Core samples			Pit
		1	2	3		1	2	3	
0	BD								DR,TI
25		*	*	*					
30	BD								DR,TI
60	BD								DR,TI
75		*	*	*					
90	BD								DR,TI
130	BD								
150		*	*	*	0-1,3,15		3,15	3,15	DR,TI
300		*	*	*			3,15	3,15	
500		*	*	*			3,15	3,15	

Notes:

H.C. = hydraulic conductivity tests

DR = Double ring infiltrometer test

TI = tension infiltrometer test

* = Full textural and bulk density analysis

BD = Bulk density analysis only

0-1 = Water retention characteristic over 0 to 1 bar

3,15 = Water retention points at 3 bar and 15 bar

Table 5 summarizes the mean soil texture and bulk density recorded at the various sample depths in the profile. The available water capacity (AWC) at each depth, as calculated by the difference in volumetric water content at 0.1 and 15 bars, is also shown. The AWC for unsampled depths is estimated as an average of the nearest sampled depths above and below. The total AWC of the 8 m profile was thus estimated to be 1568 mm.

Table 5. Soil texture, bulk density and available water capacity (AWC) at site 1.

Depth (cm)	Horizon depth (mm)	Sand (%)	Silt (%)	Clay (%)	Bulk density (g cm^{-3})	AWC (cm^3 cm^{-3})	AWC (mm)
25	375	49	23	28	1.159	0.144	54
50	250						37
75	250	50	24	26	1.190	0.147	37
100	250						37
125	250						48
150	250	41	38	21	1.233	0.191	48
175	250						48
200	625						119
300	1000	44	40	16	1.234	0.19	190
400	1000						190
500	1000	54	40	6	1.244	0.19	190
600	1000						190
700	1000						190
800	1000						190
Total							1568

A graphical representation of mean trends in soil texture down the profile is illustrated in figure 11. There is a marked decline in the clay with increasing depth, with corresponding increases in both silt and sand.

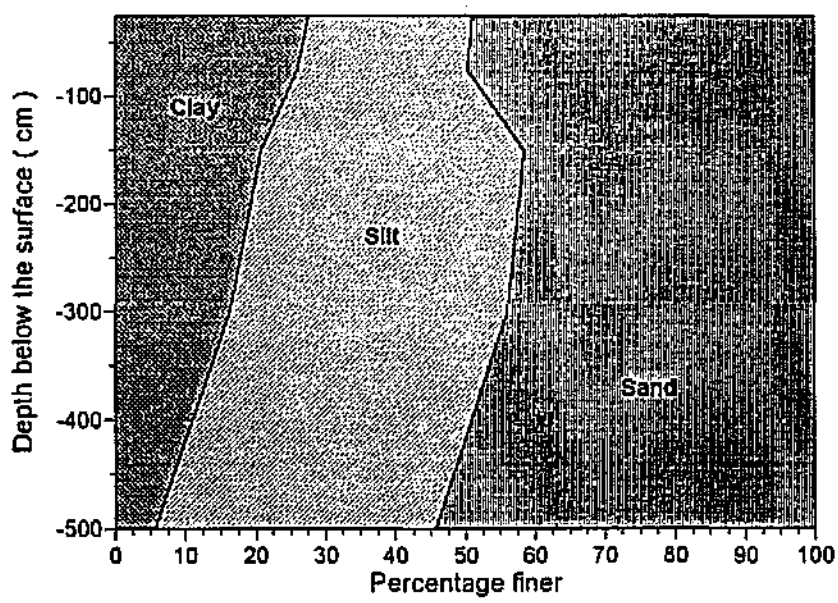

Figure 11. Changes in the mean proportions of clay, silt and sand recorded at various depths in the profile at site 1.

The relation between soil water content and matric pressure head at three sample depths is shown in figure 12.

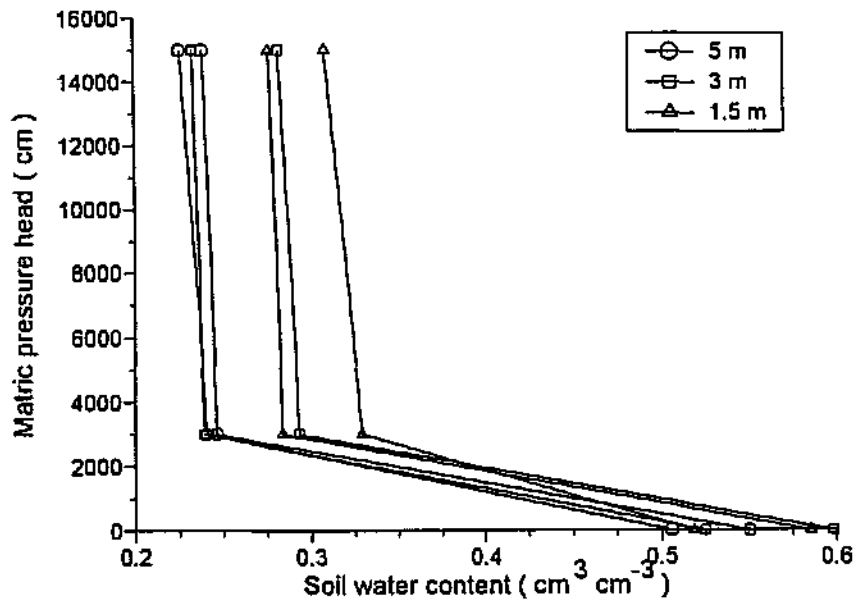

Figure 12. The relation between soil water content and matric pressure head recorded for soil from three depths in the profile at site 1.

Figure 13 illustrates the profile trends in moisture contents corresponding to tensions of 0.1 bar and 15 bar. The data from depths of 25, 75 and 150 cm were derived from a regression model relating soil texture to water contents at 0.1 and 15 bars. Figure 13 also shows the porosity of the soil at each measurement depth, indicating the water content under saturated conditions.

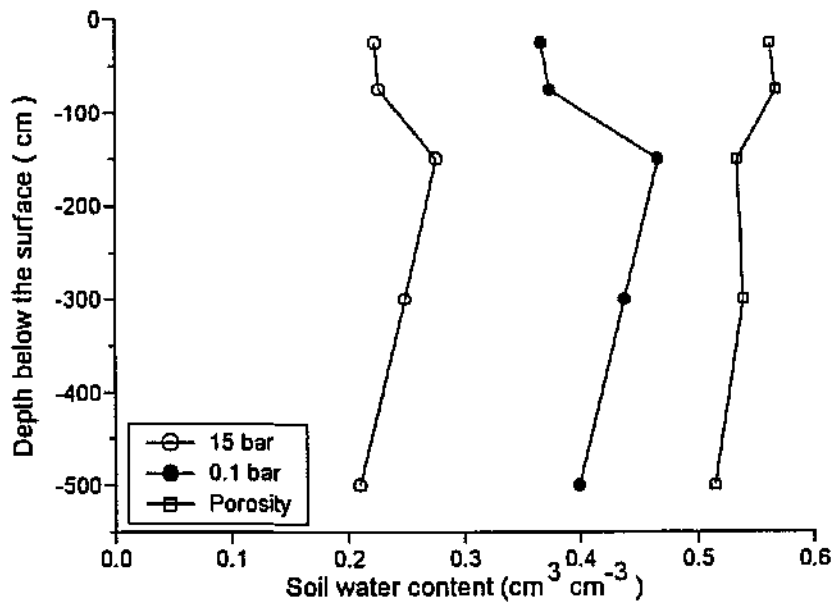

Figure 13. *Site 1 Profile trends in available water capacity, as illustrated by the water contents corresponding to 0.1 bar and 15 bar tensions. The soil porosity at each measurement depth is also indicated.*

Figure 14 shows hydraulic conductivity recorded at five depths in the profile down to 140 cm, based on *in situ* double-ring ponded infiltration and tension infiltrometer tests, as well as controlled outflow cell tests in the laboratory. The fact that the conductivity at saturation is substantially greater than at low tensions of 1 bar indicates significant macro-pore soil structure enabling rapid infiltration even during intense rainfall events.

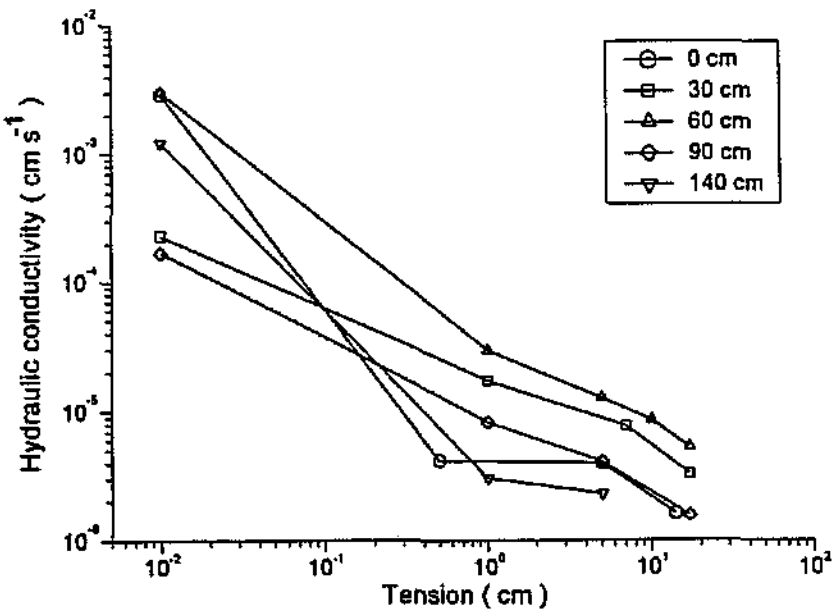

Figure 14. The relation between soil water tension and hydraulic conductivity at site 1.

Table 6 summarizes the calculated inward fluxes of soil water.

Table 6. A summary of the estimated fluxes at site 1.

Flow direction	Depth (cm)	Outer tube water content	Inner tube water content	Hydraulic gradient	Hydraulic conductivity (mm hr^{-1})	Daily flux into element (l day^{-1})
5 up	25	0.38		-9.2	2.4E-3	-8.7
	50	0.36		2.8	3.2E-3	4.4
	100	0.41		-51.7	2.9E-3	-3.5
	150	0.27		-2.0	1.1E-5	-0.01
	200	0.26		15.4	3.0E-5	0.4
	300	0.27		4.2	2.8E-4	2.6
	500	0.34		-1.27	6.0E-3	-0.6
	800	0.39				
7 up	25	0.38		0.53	4.1E-3	0.6
	50	0.40		-7.7	2.2E-3	-1.9
	100	0.36		-282.1	2.4E-4	-1.0
	150	0.22		90.2	3.1E-7	1.0
	200	0.22		126.7	2.7E-3	117.2
	300	0.36		-2.2	3.8E-3	-2.0
	500	0.37		-2.0	4.7E-3	-1.9
	800	0.38				~
NET	25					0.3
	50					6.5
	100					0.5
	150					2.7
	200					53.0
	300					1.1
	500					~
	800					
					Total	64

The soil water fluxes were predominantly in the vertical direction with very low lateral fluxes. There was evidence of significant quantities of water being drawn

upwards from the 800 cm level. This was especially true in the vicinity of tube 7. The movement of soil water was predominantly into the 100 to 200 cm layer. The estimate of the net amount of soil water moving into the 100 - 200 cm layer and not exiting these layers (therefore being taken up by the trees) amounts to some 64 litres per day per tree, amounting to approximately 3.9 mm per day over the area served by the four trees. The flux estimate in this zone was strongly influenced by high hydraulic gradients observed in a single access tube (tube 7).

4.1.8 Soil resistance measurements

Figure 15 illustrates the variation in soil resistance measured along a transect centred on the site. The readings suggest the presence of relatively moist soil down to 40 m below the surface, but with significant spatial heterogeneity.

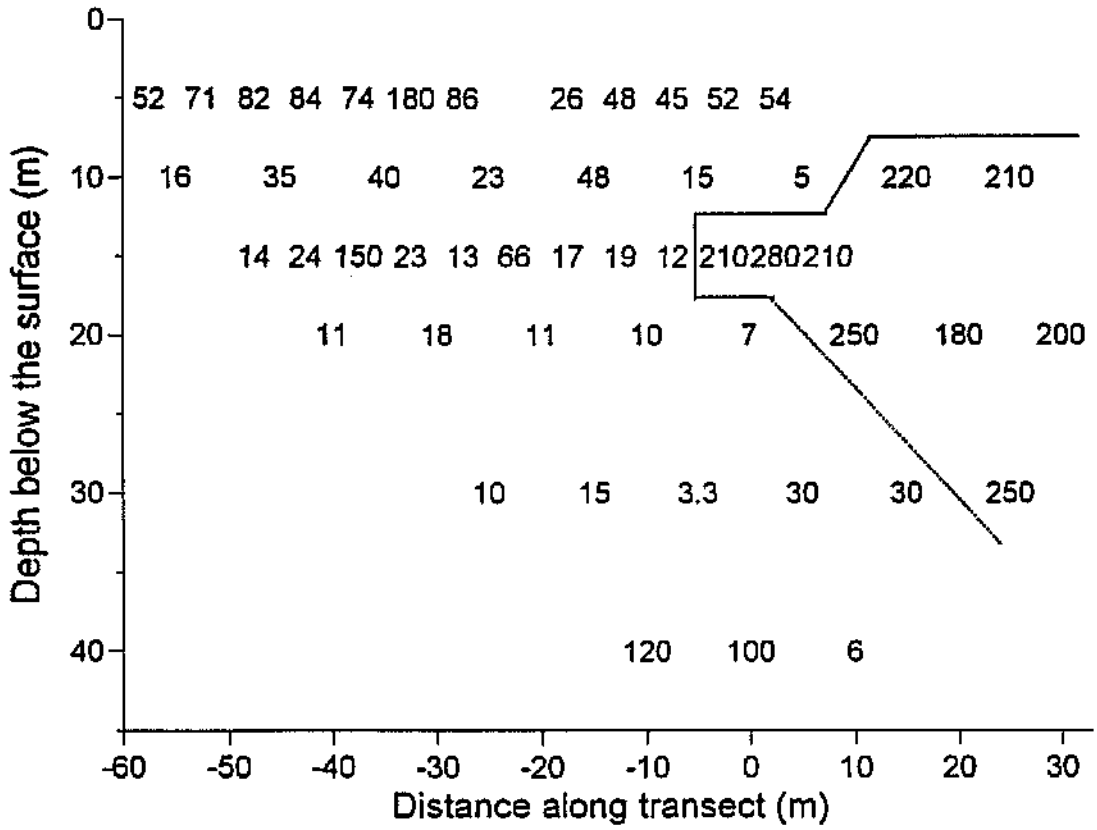

Figure 15. A two-dimensional map of profile soil resistance readings (ohm-cm) recorded at site 1. The dotted line is thought to enclose a region of partially decomposed granite.

4.1.9 Summary

It is remarkable that the trees at this site did not experience a high degree of stress due to soil water deficits. The study commenced at a time of severe drought following the particularly dry 1991/92 summer (approximately 700 mm rainfall). The plastic sheeting prevented soil water recharge for 13 months, which included the entire duration of the following 1992/93 summer. The annual pattern of daily sap flow displayed seasonal changes, but exhibited no progressive decline which could be attributed to increasing soil water deficit. Leaf area index remained relatively constant. Pre-dawn XPP data showed that lowest potentials barely exceeded -0.7 MPa. Prevention of soil water recharge resulted in more negative water potentials in the trees under plastic than was recorded in control trees nearby. However, the greatest difference only amounted to approximately -0.3 MPa. The stomatal conductance and growth data likewise indicate the absence of marked stress in the trees. The reason for this remarkable resistance to the induced drought is apparent from figure 8, which indicates the ability of this species to take up soil water from depths to 8 m and deeper.

Comparison of total sap flow over the study period (1325 mm) against apparent soil water abstraction from the 8 m profile (607 mm) suggests that only 46% of the water used by the trees originated from soil to this depth. The remainder (718 mm) is hypothesized to come either from yet deeper levels in the profile, or else through lateral and vertical movement into the monitored volume of soil in response to gradients in soil water potential. The pattern of soil drying shown in figure 10

certainly suggests that soil water may be abstracted from levels deeper than 8 m. The analysis of lateral or vertical soil water influx showed that lateral flux was insignificant, but that appreciable vertical flux took place especially from the 800 cm level towards the 100-200 cm level. Theoretically, the sum of this flux (3.9 mm per day) and the apparent soil water uptake (1.56 mm per day) should not exceed the tree water use (3.4 mm per day). The fact that it does suggests that the estimate may be overestimated. As noted earlier, it was strongly influenced by large hydraulic gradients observed in a single access tube, and the limited sampling may have led to an inadequate description of the mean vertical flux. The results nevertheless indicate the possibility of significant downward movement of water following rainfall, and upwards movement during dry weather, which is likely to supplement the soil water availability within the rooting zone.

The relation between declining transpiration rate and soil water availability could not be established at this site, in view of the extremely deep soil water abstraction and the failure of the treatment to induce significant soil water deficits within the rooting zone.

4.2 Frankfort site 2

4.2.1 Sap flow measurements

A summary of various tree characteristics relating to the calculation and interpretation of sap flow is shown in table 7.The mean daily water use of the sample trees at site 2 for the period 1 June 1992 to 9 June 1993 is shown in figure 16. Daily water use averaged approximately 70 litres per day between the summer months of September to January. A noticeable increase was evident soon after the plastic sheeting was removed from this site (15 January 1993), suggesting that soil water recharge resulted in a rapid increase in transpiration rate. Peak daily water use exceeded 140 litres per day, but this was equivalent to only 4 mm in view of the lower density of trees.

Table 7. A summary of age, height, diameter at breast height (DBH), leaf area, sapwood moisture fraction, sapwood density and wound width of all four sample trees recorded at site 2 at the conclusion of the study in July 1993. Standard deviations appear in brackets. Mean leaf areas were estimated by stripping all leaves from the sample trees and estimating total area from total mass using the relation determined from a sub-sample of leaves.

	Frankfort site 2
Age (years)	10
Mean height (m)	34.3 (1.15)
Mean DBH (cm)	29.7 (4.53)
Mean leaf area per tree (m^2)	71.4 (36.86)
Mean sapwood moisture fraction	1.13 (0.281)
Mean wood density (g cm^{-3})	0.49 (0.073)
Mean wound width (mm)	2.88 (0.390)
Mean ground area per tree (m^2)	31.8

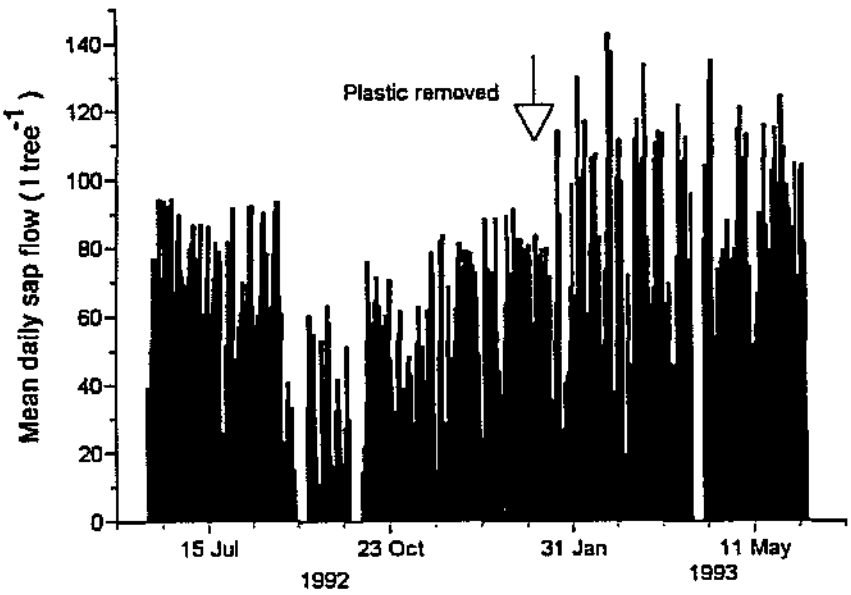

Figure 16. Total daily sap flow (mean of four trees) recorded at site 2.

4.2.2 Pre-dawn xylem pressure potential

Measurements of leaves from the site 2 trees (figure 17) indicate more negative XPP than was recorded at site 1, but a similar trend over time. Two data points in October departed from the trend, but were both recorded on days when the leaves were wet due to rainfall during the night. Experience has shown that such conditions result in significantly less negative pre-dawn readings. The plastic sheeting at site 2 was removed on 15 January 1993. With the resumption of rainfall infiltration into the soil, pre-dawn XPP readings became less negative, indicating that a degree of physiological stress was being experienced by the trees prior to removal of the plastic sheeting.

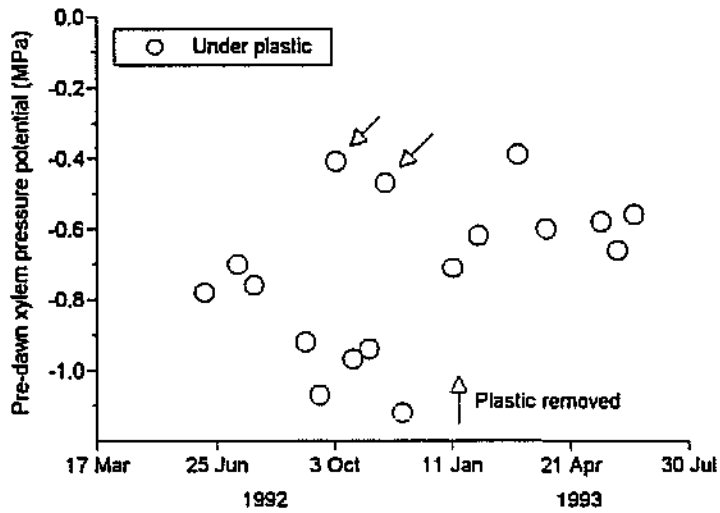

Figure 17. Site 2. The trends in mean pre-dawn xylem pressure potential recorded in four sample trees before and after the plastic sheeting was in place. The arrows indicate sample days when the canopy was wet.

4.2.3 Leaf area index

The LAI recorded at site 2 is lower than at site 1 (figure 18), as a result of the lower tree density in this thinned stand. The readings were more variable than at site 1, and this is attributed to changes in light intensity during the greater time interval between above and below canopy readings at this site. Above canopy readings had to be taken in a clearing a few hundred metres from the site, and so the time required to record a complete set of data was longer than at site 1, providing more opportunity for light intensity to change. There is again no indication of a marked

decline in LAI for the period the plastic sheeting was in place.

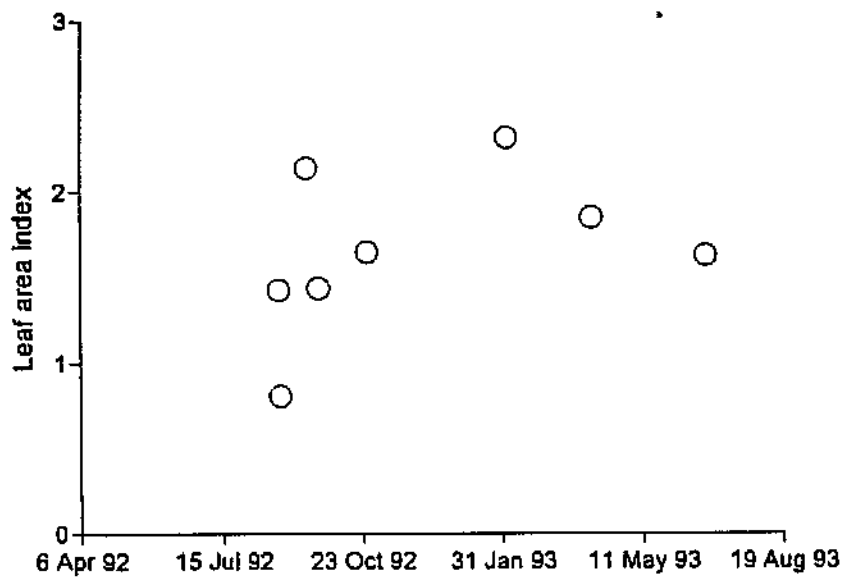

Figure 18. The trend in leaf area index recorded at site 2.

4.2.4 Apparent soil water abstraction

Table 8 shows the calibration equations determined for soils at 25, 100 and 300 cm below the surface. As at site 1, the calibration equation for 25 cm was used at 50 cm, the 100 cm calibration was used at 75, 125 and 150 cm, and the 300 cm calibration was also applied to 175, 200, 400, 500, 600, 700 and 800 cm below the surface.

Table 8. Calibration equations pertaining to three soil horizons at site 2. R = counts at the sample depth; Rw = counts under water.

Depth (cm)	Calibration equation
25	$\theta = 0.819 * R/Rw - 0.057$
100	$\theta = 0.806 * R/Rw - 0.1077$
300	$\theta = 0.790 * R/Rw - 0.0971$

Figure 19 shows the pattern of change in volumetric soil water contents between 1 June 1992 and 22 December 1992. In light of the relatively small changes in soil water at this site, it was decided to remove the plastic sheeting in January 1993 to observe the physiological response of the trees to the sudden increase in the availability of soil water. The lines without symbols in figure 19 show the changes in the soil water content which took place in the following four months.

Table 9 shows the apparent soil water uptake recorded at each measurement depth between 1 June 1992 and 22 December 1992. Assuming the absence of significant soil water movement as a result of potential gradients, the trees obtained only 45% of their water requirement from the first 8 m of soil.

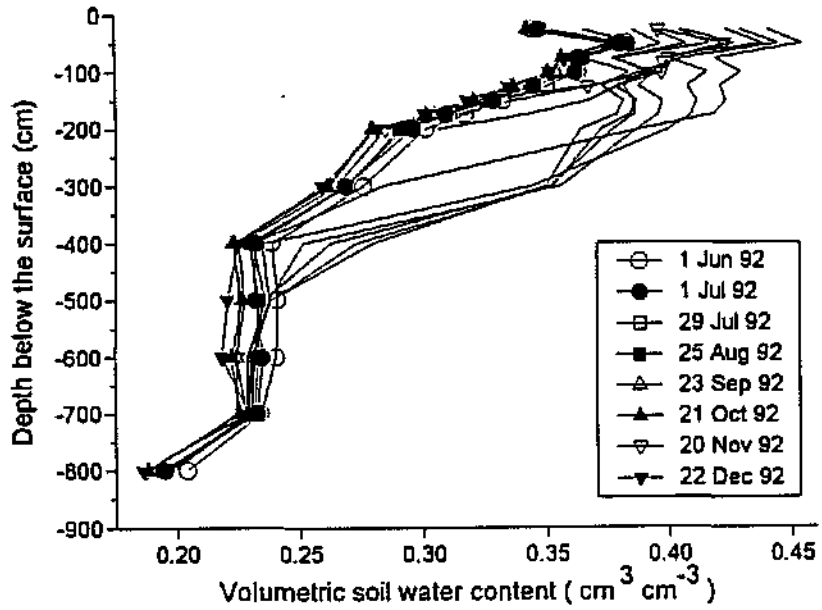

Figure 19. Changes in volumetric soil water content recorded in the soil beneath the sample at site 2. Lines without symbols show changes after the plastic sheeting was removed. Rainfall totalled 594 mm after this time.

Table 9. The apparent soil water uptake at site 2 recorded at each measurement depth between 1 June 1992 and 22 December 1992 (205 days). Total uptake is compared to sap flow over the same period.

Depth (cm)	Soil water (cm^3 cm^{-3}) (1-6-92)	Soil water (cm^3 cm^{-3}) (22-12-92)	Difference (cm^3 cm^{-3})	Horizon depth (mm)	Soil water uptake (mm)
25	0.345	0.345	-0.001	375	0
50	0.384	0.380	0.004	250	1
75	0.366	0.358	0.008	250	2
100	0.364	0.352	0.012	250	3
125	0.351	0.335	0.016	250	4
150	0.333	0.318	0.015	250	4
175	0.317	0.301	0.016	250	4
200	0.301	0.282	0.020	625	13
300	0.276	0.259	0.017	1000	17
400	0.238	0.225	0.014	1000	14
500	0.241	0.220	0.021	1000	21
600	0.240	0.218	0.022	1000	22
700	0.234	0.229	0.004	1000	4
800	0.204	0.186	0.018	1000	18
Total					127
			Total sap flow (mm)		339
			% of total sap flow		37

4.2.5 Lateral and vertical soil water influx

Table 10 summarizes the set of *in-situ* and laboratory measurements recorded at this site.

Table 10. A summary of soil physical and hydraulic property tests performed at site 2, Frankfort Plantation.

Depth	Texture and bulk density				Water retention				H.C.
	Pit	Core samples			Pit	Core samples			Pit
		1	2	3		1	2	3	
0	BD								DR,TI
25		*	*	*					
30	BD								DR,TI
60	BD								DR,TI
75		*	*	*					
90	BD								DR,TI
130	BD								DR,TI
150		*	*	*			3,15		
300		*	*	*			3,15	3,15	
500		*	*	*			3,15	3,15	

Notes:

H.C. = hydraulic conductivity tests

DR = Double ring infiltrometer test

TI = tension infiltrometer test

3,15 = Water retention points at 3 bar and 15 bar

* = Full textural and bulk density analysis

BD = Bulk density analysis only

0-1 = Water retention characteristic over 0 to 1 bar

Table 11 summarizes the soil texture and bulk density recorded at various depths in the profile. The available water capacity (AWC) at each measurement depth, as calculated by the difference in volumetric water content at 0.1 and 15 bars, is also shown. The AWC for unmeasured depths is estimated by averaging over the nearest measured depths above and below the depth in question. The total AWC of the 8 m profile was thus estimated to be 1707 mm.

Table 11. Soil texture, bulk density and available water capacity (AWC) at site 2.

Depth (cm)	Horizon depth (mm)	Sand (%)	Silt (%)	Clay (%)	Bulk density (g cm^{-3})	AWC (cm^3 cm^{-3})	AWC (mm)
25	375	60	17	23	1.192	0.183	69
50	250						50
75	250	50	22	28	1.239	0.21	53
100	250						53
125	250						50
150	250	50	30	20	1.251	0.201	50
175	250						50
200	625						118
300	1000	54	31	15	1.367	0.188	188
400	1000						198
500	1000	46	43	11	1.329	0.207	207
600	1000						207
700	1000						207
800	1000						207
Total							1707

A graphical representation of trends in soil texture down the profile is illustrated in figure 20. As in site 1, there is a marked decline in clay content with depth. The increase in silt content with depth is especially evident at this site.

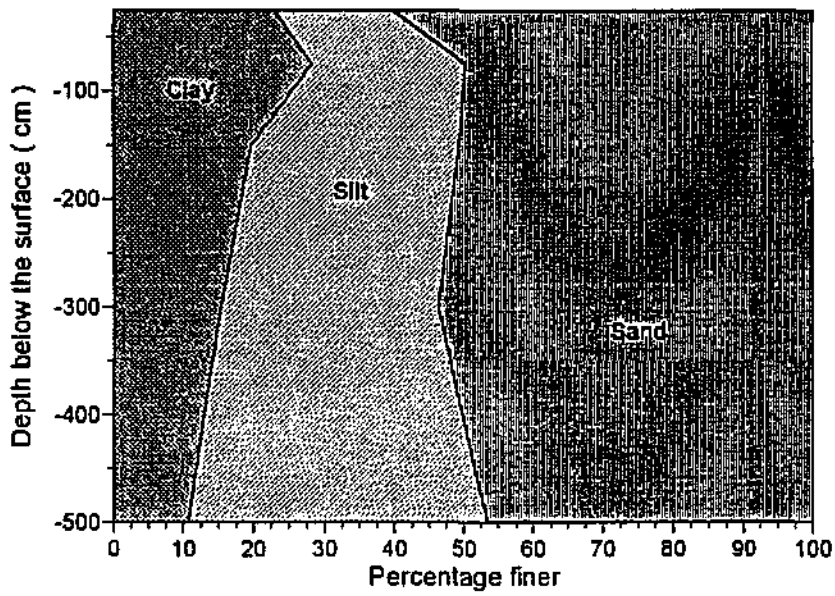

Figure 20. Changes in the mean proportions of clay, silt and sand recorded at various depths in the profile at site 2.

The water retention characteristics of soil samples at 1.5, 3 and 5 m depths was recorded using the controlled outflow cell method. The relation between soil water content and matric pressure head is shown in figure 21.

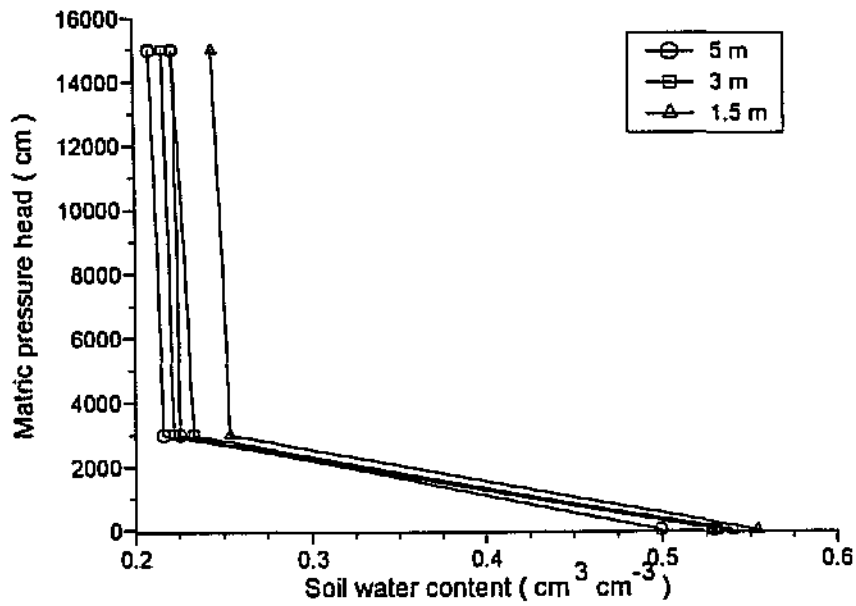

Figure 21. The relation between soil water content and matric pressure head recorded for soil from three depths in the profile at site 2.

Figure 22 illustrates the profile trends in moisture contents corresponding to tensions of 0.1 bar and 15 bar. The data from depths of 25, 75 and 150 cm were derived from a regression model relating soil texture to water contents at these tensions. Figure 22 also shows the porosity of the soil at each measurement depth, indicating the water content under conditions of saturation.

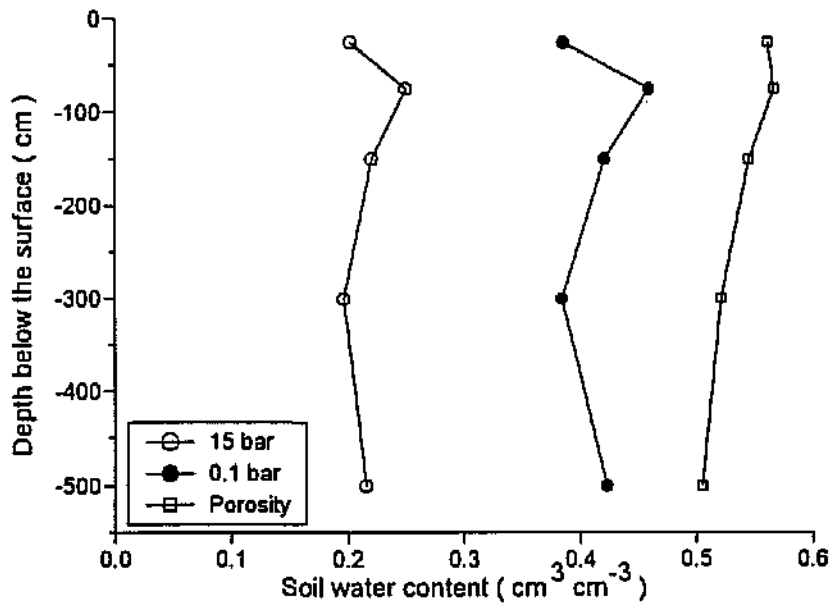

Figure 22. Site 2 profile trends in available water capacity, as illustrated by the water contents corresponding to 0.1 and 15 bar tensions. The soil porosity at each measurement depth is also indicated.

Figure 23 shows hydraulic conductivity recorded at five depths in the profile down to 140 cm. The data are based on *in-situ* double-ring ponded infiltration and tension infiltrometer tests, as well as controlled outflow cell tests in the laboratory.

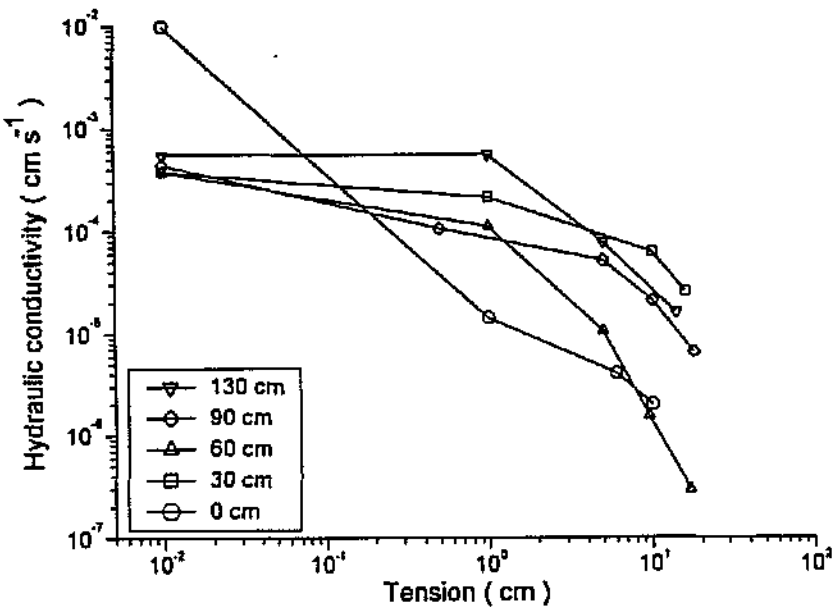

Figure 23. The relation between soil water tension and hydraulic conductivity.

Table 12 summarizes the estimated fluxes at site 2.

Table 12. A summary of estimated soil water fluxes at site 2.

Flow direction	Depth (cm)	Outer tube water content	Inner tube water content	Hydraulic gradient	Hydraulic conductivity (mm hr^{-1})	Daily flux into element (l day^{-1})
3 to 4	25	0.36	0.34	0.22	2.1E-3	0.01
	50					~
	100	0.44	0.40	0.16	2.2E-2	0.09
	150	0.36	0.38	-0.14	2.1E-3	-0.03
	200					~
	300	0.36	0.30	0.78	2.8E-3	0.26
	500	0.27	0.24	4.88	3.7E-6	~
	800	0.20	0.21	~		~
10 to 5	25	0.35	0.34	0.12	9.0E-4	~
	50	0.42	0.37	0.29	5.0E-3	0.05
	100	0.43	0.41	0.08	9.8E-3	0.04
	150	0.36	0.36	~	~	~
	200	0.38	0.27	2.6	4.2E-3	0.08
	300	0.34	0.20	15.5	1.1E-3	2.40
	500	0.28	0.26	~	~	~
	800	0.19	0.32	-20.9	1.4E-4	-0.57
4 up	25	0.33		11.78	5.0E-3	5.4
	50	0.38		-2.35	6.2E-3	-1.6
	100	0.38		0.90	3.5E-3	0.9
	150	0.37		-2.10	2.4E-3	-1.6
	200	0.35		-5.9	2.3E-3	-1.2
	300	0.30		-33.8	2.1E-3	-0.7
	500	0.24		35.0	4.3E-4	0.1
	800	0.22				
5 up	25	0.34		4.0	5.0E-3	4.1
	50	0.37		1.31	6.2E-3	3.2
	100	0.41		2.70	3.5E-3	-3.6
	150	0.36		347.2	2.4E-3	-7.3
	200	0.27		-124.0	2.3E-3	-0.2
	300	0.20		52.8	2.1E-3	1.1
	500	0.26		79.0	4.3E-4	0.2
	800	0.32				

7 up	25	0.35		0.57	1.4E-3	3.6
	50	0.37		2.77	6.2E-3	16.8
	100	0.44		-3.05	3.5E-3	-12.2
	150	0.37		-0.20	2.4E-3	-1.1
	200	0.36		-1.59	2.3E-3	-1.1
	300	0.33		-17.1	2.1E-3	-1.8
	500	0.26		-48.8	4.3E-4	-0.01
	800	0.20				~
NET	25					4.4
	50					6.7
	100					0.8
	150					2.5
	200					2.5
	300					0.4
	500					1.2
	800					
					Total	19

This site was characterized by relatively moist soils between 25 and 100 cm, and becoming progressively dryer between 100 and 800 cm. The movement of soil water was predominantly vertical with very low lateral fluxes. There was some evidence of water moving upwards from the 800 cm level, although the flux was not high and only manifested in the vicinity of tube 5. The estimate of the net amount of soil water moving into the 25 to 100 cm layer and not exiting these layers (therefore being taken up by the trees) amounted to 19 litres per day per tree. This approximates 1.2 mm per day over the representative soil volume serving the four trees.

4.2.6 Soil resistance measurements

Figure 24 illustrates the variation in soil resistance measured along a transect

centred on the site. The readings suggest a variable bedrock stratum below 30 m, and distinct bands of relatively wet and dry material in a spatially heterogeneous subsoil.

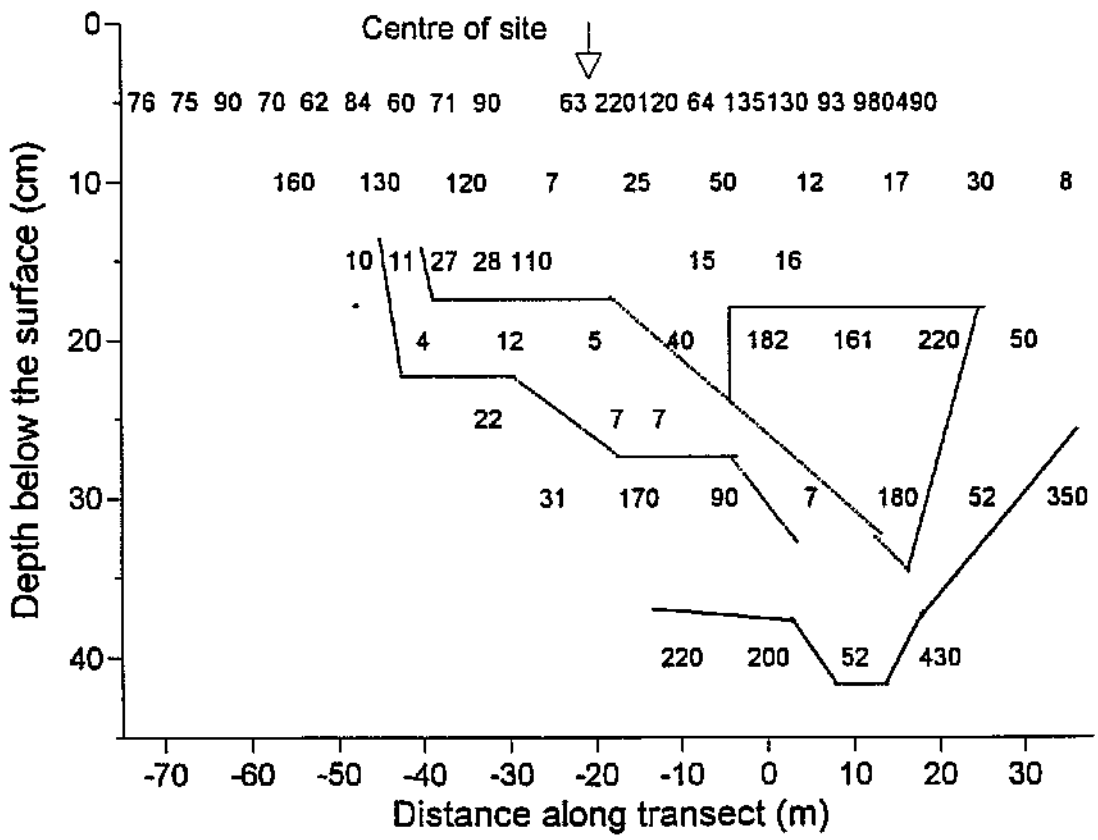

Figure 24. A two-dimensional map of profile soil resistance readings (ohm-cm) recorded at site 2. Dotted lines enclose regions of especially high and low soil resistance.

4.2.7 Summary

The sap flow data show a distinct increase immediately after the plastic sheeting was removed, showing that the trees were experiencing sufficient stress during the first half of the summer to reduce transpiration rates by approximately 20-25 %.This conclusion is consistent with the XPP data, which were indicative of a moderate degree of stress developing in the trees just prior to the plastic sheeting being removed. The LAI data indicated no marked change in response to the drying soil. The soil water abstraction pattern indicated relatively small changes in soil water contents. The sum of these changes accounted for only 37% of the measured sap flow in the trees, pointing to the importance of deeper soil water reserves to the trees. Soil resistance measurements revealed the depth of bedrock to be below 30 m, and showed the presence of relatively wet subsoil. The analysis of soil water contents and hydraulic gradients once again revealed insignificant lateral flux towards the sample trees. Some evidence from the vicinity of tube 5 pointed to a vertical flux, predominantly from the 800 cm level towards the 25-100 cm level. This flux amounted to 1.2 mm per day, which is close to the difference between the tree water use (1.65 mm per day) and the apparent soil water uptake (0.62 mm per day). This result raises the possibility that upwards flux may have sufficiently augmented the soil water content of the monitored profile to meet the water requirement of the trees. This possibility should be treated with caution, however, in view of the fact that the flux was not high, and was manifest only in the vicinity of tube 5. In view of the evidence for soil water uptake down to 8 m by the younger trees at site 1, one must presume that older trees are very likely to send roots below 8 m to secure

additional water.

As was the case at site 1, I concluded that it was not possible to relate transpiration reduction to soil water availability, due to relatively low levels of stress in the trees and to much uncertainty over the rooting depth and the total quantity of water available to the trees.

4.3 Legogote site 3

4.3.1 Sap flow measurements

A summary of various tree characteristics relating to the calculation and interpretation of sap flow rates is shown in Table 13. Mean daily sap flow is shown in figure 25, while the weekly rainfall recorded prior to the plastic sheeting being laid out is shown in figure 26.

Table 13. A summary of age, height, diameter at breast height (DBH), sapwood moisture fraction, sapwood density and wound width of all four sample trees recorded at site 3 at the conclusion of the study in December 1995. Standard deviations appear in brackets.

	Legogote site 3
Age (years)	6
Mean height (m)	16.02 (0.738)
Mean DBH (cm)	14.77 (0.430)
Mean sapwood moisture fraction	0.695 (0.034)
Mean wood density (g cm^{-3})	0.630 (0.034)
Mean wound width (mm)	3.30 (0.543)
Mean ground area per tree (m^2)	13.1

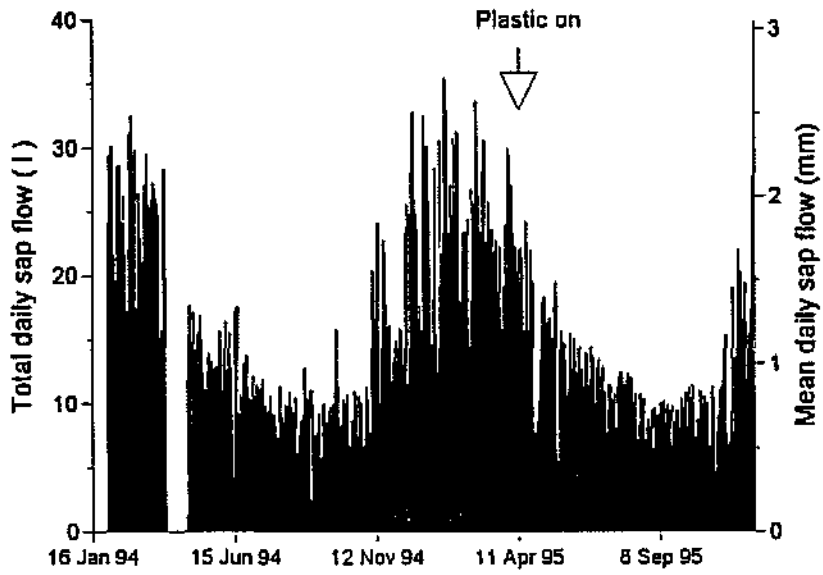

Figure 25. Total daily sap flow (mean of four trees) recorded at site 3.

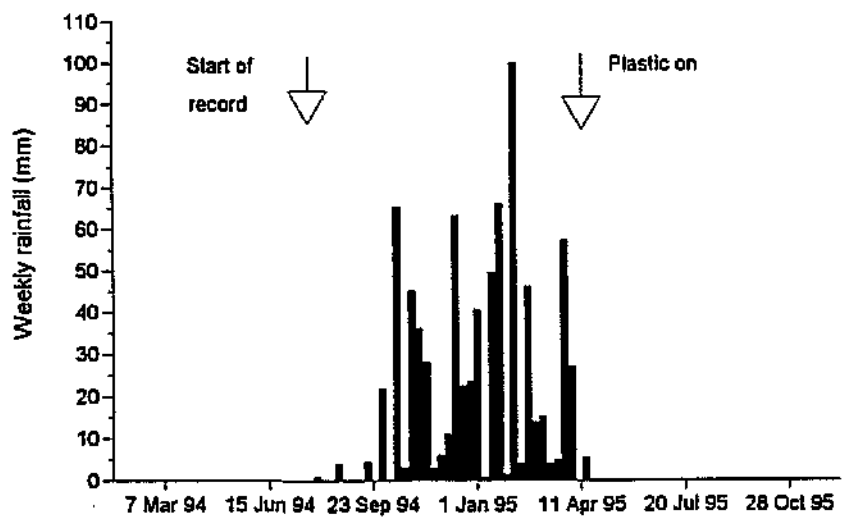

Figure 26. Weekly rainfall recorded at site 3 prior to the plastic sheeting being laid out.

Sap flow rates show a similar pattern of seasonal variation to that recorded at site 1, with maximum rates occurring in mid-summer and minimum rates at the end of the winter dry season. However, the measured rates at site 3 were less than half those at site 1, giving rise to particularly low winter rates of less than 1 mm per day. Choosing the most appropriate time to lay out the plastic sheeting proved to be a difficult decision. At the start of the study, the sample trees were already displaying symptoms of severe stress and the soil profile appeared to be relatively dry. It was felt therefore that the soil should be allowed to recharge so that the relation between transpiration rate and soil water availability could be observed over a wide range of water availability. The sheeting was therefore only laid out in April 1995, after the bulk of the summer rains had fallen. The winter decline in transpiration therefore appeared to very similar to that recorded the previous winter. A rise in daily sap flow was recorded towards the end of the study, and is attributed to rainfall leaking through the deteriorating plastic sheeting during heavy rainfall.

4.3.2 Xylem pressure potential

The trends in both pre-dawn and mid-day xylem pressure potential are shown in figure 27. The trees experienced very high levels of stress up to 23 September 94, with pre-dawn XPP becoming only slightly less negative than the mid-day readings. This indicates that the normal night-time equilibration of xylem water potential could not take place due to insufficient soil water. The rains which fell after 23 September brought about a quick return to XPP patterns typical of unstressed trees, with pre-

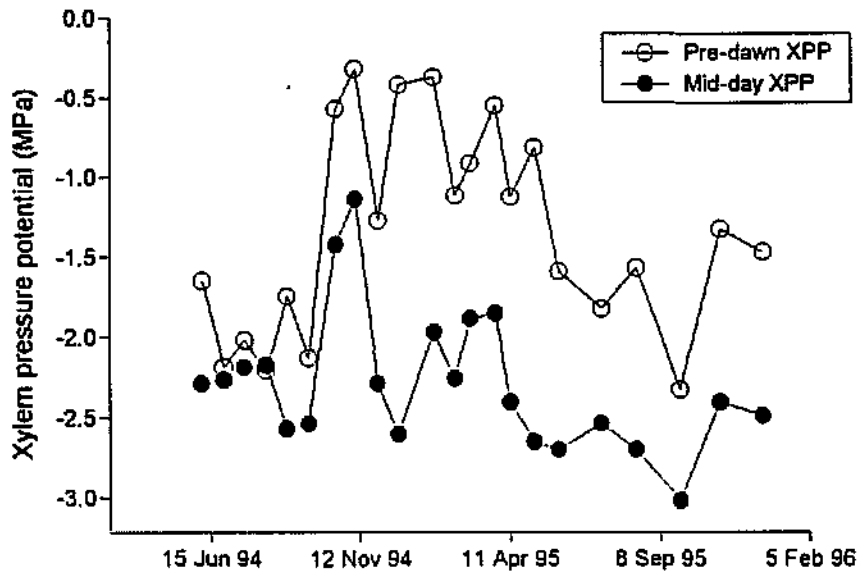

Figure 27. Site 3. The trends in mean pre-dawn and mid-day xylem pressure potential recorded in four sample trees under plastic sheeting.

dawn readings of approximately -0.4 to -0.8 MPa. However, these readings gradually became more negative during the 1995 winter, converging towards (but not reaching) the mid-day readings at the end of winter. The trend towards more negative mid-day potentials is interesting, and may indicate a physiological adaption in the leaves. A degree of recovery is indicated by the last two readings, probably brought about by leaks in the plastic sheeting.

4.3.3 Leaf area index

Figure 28 shows the trend in leaf area index recorded at site 3. There is a clear

reduction in LAI at the time of severe stress up to September 1994, showing that the trees were resorting to leaf shedding to reduce the transpirational demand. Partial recovery took place during the following summer months, as rainfall and an improved water status in the trees permitted the growth of new leaves. LAI did not show a marked decline during the winter of 1995, suggesting that the level of stress was not as severe as at the end of the previous winter. The XPP data appear to support this conclusion.

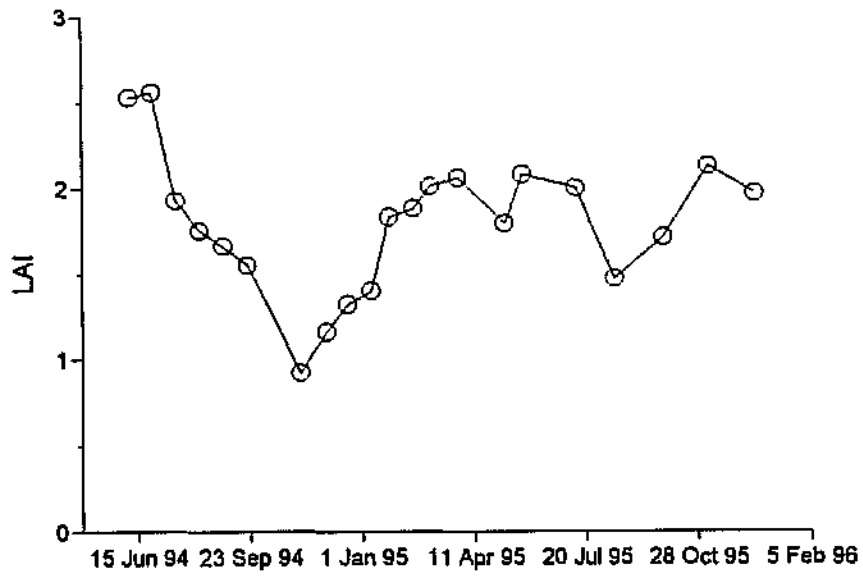

Figure 28. The trend in leaf area index (LAI) recorded at site 3.

4.3.4 Leaf stomatal conductance

Figure 29 shows mean stomatal conductance recorded at site 3. As was to be

expected, conductances were extremely low at the end of the first winter. These became significantly higher during the following summer months as rainfall improved the water status of the trees. However, peak conductances of only 200 m mol m^{-2} s^{-1} were recorded, corresponding to the lowest readings measured at site 1. This large difference is believed to be a result of adaption by the Legogote trees to the regular soil water deficits experienced each winter.

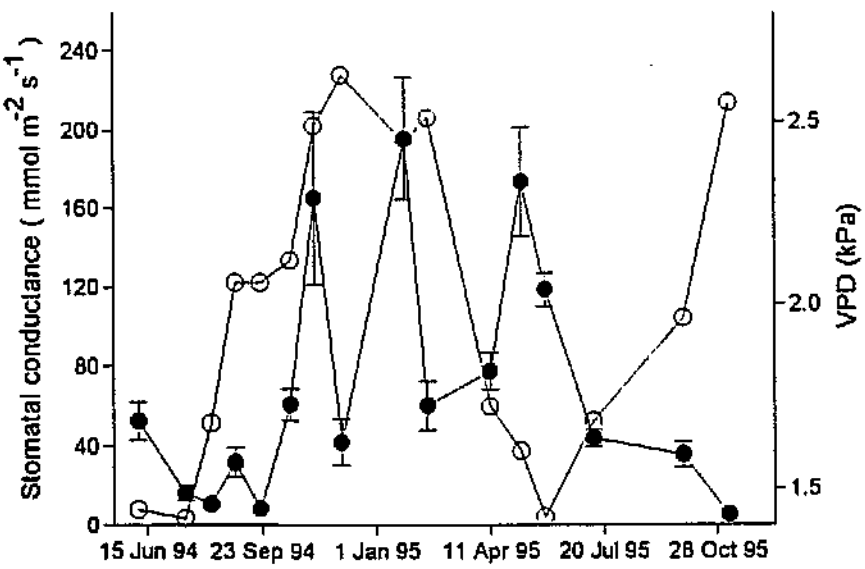

Figure 29. The trend in stomatal conductance (mean of 12 leaves, solid symbols) recorded at 13h00 in upper canopy leaves exposed to direct sunlight at site 3. Mean vapour pressure deficit is indicated by open symbols.

4.3.5 Trunk growth

Figure 30 illustrates changes in mean DBH and height at this site. The trend in mean DBH clearly shows two periods of slowed growth in the winter months (approximately June to October) which correspond to the times of water stress shown by the XPP data. It is most interesting to see that growth does not cease even when water stress is severe. The trend in the mean height data shows similar slowed growth during the winter months. However, there is also a pronounced slow down in mid-summer which is not reflected in diameter growth increments. It must be concluded that this reflects a natural growth rhythm.

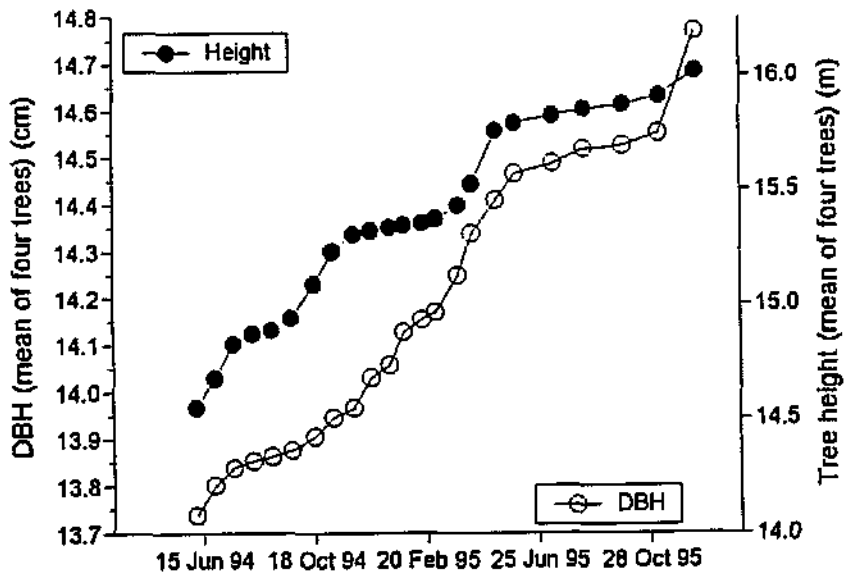

Figure 30. The trends in mean tree height and DBH recorded at site 3.

4.3.6 Apparent soil water abstraction

Table 14 shows the calibration equations pertaining to the three soil samples at site 3.

Table 14. Calibration equations pertaining to three soil horizons at site 3. R = counts at the sample depth; Rw = counts under water.

Depth (cm)	Calibration equation
25	$\theta = 0.869 * R/Rw - 0.0904$
100	$\theta = 0.818 * R/Rw - 0.1002$
300	$\theta = 0.835 * R/Rw - 0.0871$

Figure 31 shows the pattern of change in volumetric soil water over the entire monitoring period from February 1994 to December 1995. Symbols have been omitted in view of the very small changes which were recorded.

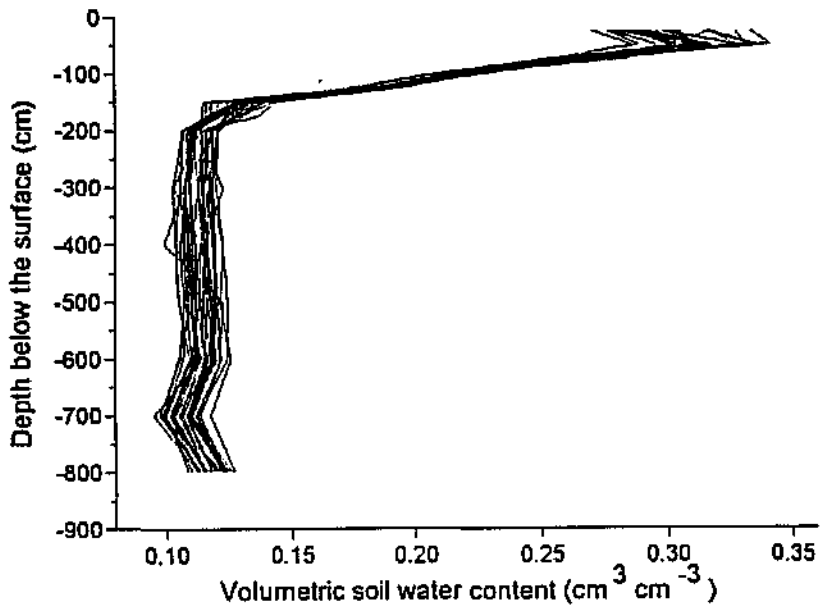

Figure 31. Profiles of volumetric soil water contents recorded at site 3.

Table 15 shows the apparent soil water uptake recorded at each measurement depth between 11 April 1995 and 7 November 1995. Assuming no change in soil water due to gradients in water potential, the total uptake is equivalent to 48% of measured sap flow.

Table 15. The apparent soil water uptake recorded at each measurement depth between 11 April 1995 and 7 November 1995 (211 days). Total uptake is compared to sap flow over the same period.

Depth (cm)	Soil water ($cm^3\ cm^{-3}$) (11-4-95)	Soil water ($cm^3\ cm^{-3}$) (7-11-95)	Difference ($cm^3\ cm^{-3}$)	Horizon depth (mm)	Soil water uptake (mm)
25	0.289	0.291	-0.001	375	0
50	0.314	0.316	-0.001	250	0
75	0.256	0.255	0.001	250	0
100	0.215	0.209	0.005	250	1
125	0.185	0.178	0.007	250	2
150	0.124	0.116	0.008	250	2
175	0.127	0.116	0.011	250	3
200	0.118	0.108	0.009	625	6
300	0.119	0.108	0.011	1000	11
400	0.120	0.106	0.014	1000	14
500	0.119	0.107	0.012	1000	12
600	0.118	0.106	0.013	1000	13
700	0.109	0.097	0.012	1000	12
800	0.124	0.113	0.011	1000	11
Total					87
			Total sap flow (mm)		181
			% of total sap flow		48%

4.3.7 Lateral and vertical soil water influx

Table 16 summarizes the set of *in-situ* and laboratory measurements recorded at this site.

Table 16. A summary of soil physical and hydraulic property tests performed at site 3, Legogote.

Depth	Texture and bulk density				Water retention				H.C.
	Pit	Core samples			Pit	Core samples			Pit
		1	2	3		1	2	3	
0	BD								DR,TI
25		*	*	*					
30	BD								TI
60	BD								DR
75		*	*	*					
90	BD				0-1				DR,TI
130	BD								
150		*	*	*	0-1		3,15		DR
300		*	*	*			3,15	3,15	
500		*	*	*		0-1,3,15	3,15	3,15	

Notes:

H.C. = hydraulic conductivity tests

DR = Double ring infiltrometer test

TI = tension infiltrometer test

3,15 = Water retention points at 3 bar and 15 bar

* = Full textural and bulk density analysis

BD = Bulk density analysis only

0-1 = Water retention characteristic over 0 to 1 bar

Table 17 summarizes the soil texture and bulk density recorded at various depths in the profile. The available water capacity (AWC) at each measurement depth, as calculated by the difference in volumetric water content at 0.1 and 15 bars, is also shown. The AWC for unmeasured depths is estimated as an average of the nearest measured depths above and below the depth in question. The total AWC of the 8 m profile was thus estimated to be 1505 mm.

Table 17. Soil texture, bulk density and available water capacity (AWC) at site 3.

Depth (cm)	Horizon depth (mm)	Sand (%)	Silt (%)	Clay (%)	Bulk density (g cm^{-3})	AWC (cm^3 cm^{-3})	AWC (mm)
25	375	56	17	27	1.346	0.127	48
50	250						29
75	250	38	21	41	1.210	0.106	27
100	250						27
125	250						35
150	250	40	27	33	1.369	0.138	35
175	250						35
200	625						106
300	1000	50	31	19	1.330	0.169	169
400	1000						186
500	1000	59	34	7	1.457	0.202	202
600	1000						202
700	1000						202
800	1000						202
Total							1505

Figure 32 graphically illustrates the trends in soil texture down the profile. Once again, clay content declines with depth, but at this site, the sand fraction is the one which increases substantially in the lower depths.

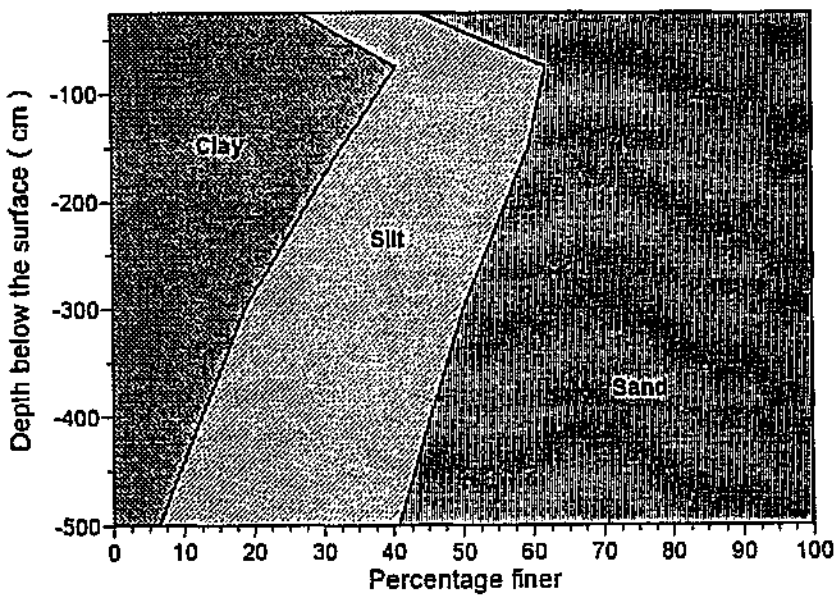

Figure 32. Changes in the mean proportions of clay, silt and sand recorded at various depths in the profile at site 3.

The water retention characteristics of soil samples at 1.5, 3 and 5 m depths was recorded using the controlled outflow cell method. The relation between soil water content and matric pressure head is shown in figure 33.

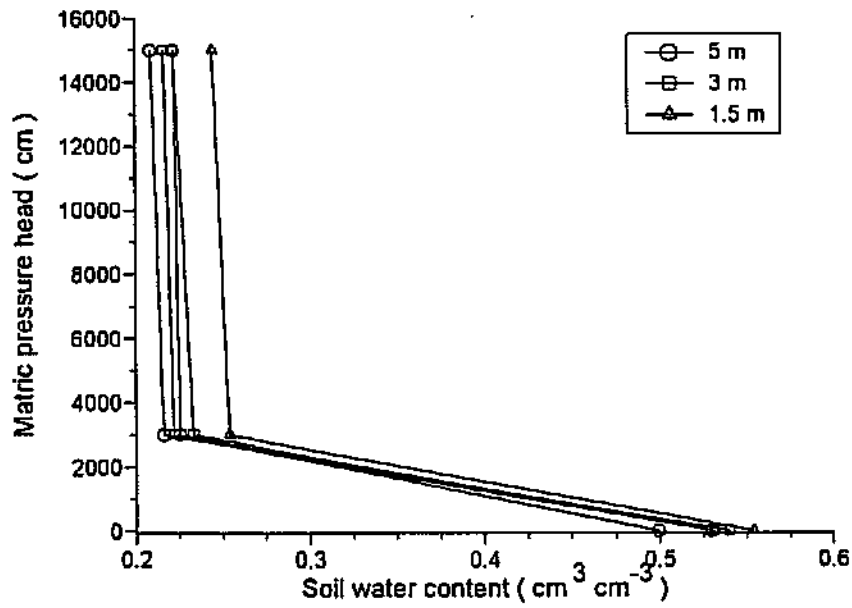

Figure 33. The relation between soil water content and matric pressure head recorded for soil from three depths in the profile at site 3.

Figure 34 illustrates the profile trends in water content corresponding to tensions of 0.1 bar and 15 bar. The data from depths of 25, 75 and 150 cm were derived from a regression model relating soil texture to water contents at these tensions. Figure 34 also shows the porosity of the soil at each measurement depth, indicating the water content under saturated conditions.

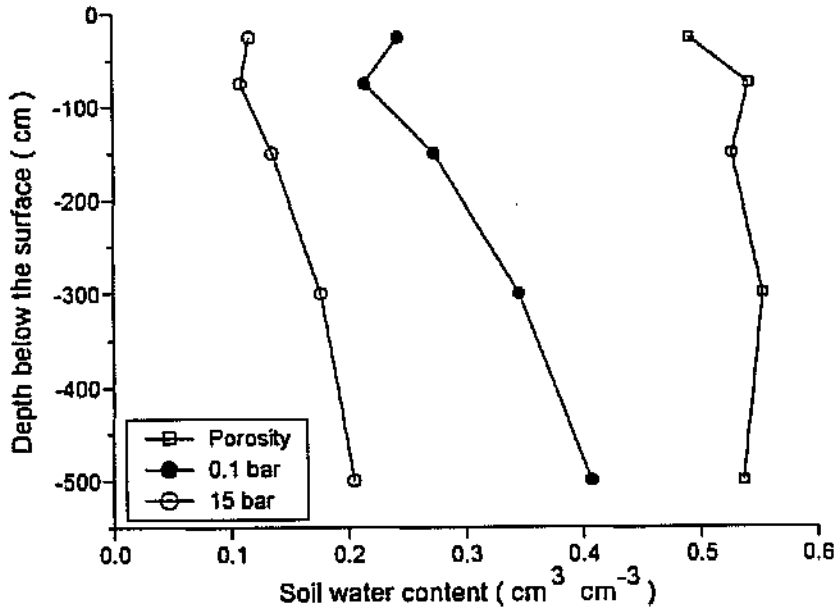

Figure 34. Site 3 profile trends in available water capacity, as illustrated by the water contents corresponding to 0.1 bar and 15 bar tensions. The soil porosity at each measurement depth is also indicated.

Figure 35 shows hydraulic conductivity recorded at five depths in the profile down to 140 cm, based on *in situ* double-ring ponded infiltration and tension infiltrometer tests, as well as controlled outflow cell tests in the laboratory.

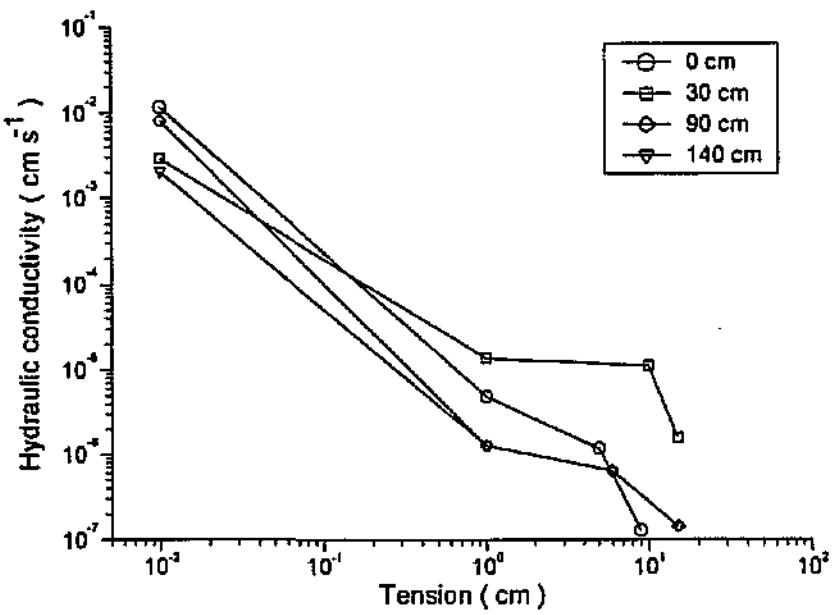

Figure 35. The relation between soil water tension and hydraulic conductivity at site 3.

Table 18 summarizes the estimated fluxes at this site.

Table 18. A summary of calculated soil water influx at site 3.

Flow direction	Depth (cm)	Outer tube water content	Inner tube water content	Hydraulic gradient	Hydraulic conductivity (mm hr-1)	Daily flux into element (l day-1)
6 - 9	25					~
	50					~
	100	0.27	0.17	1.82	2.7E-5	4.2E-3
	150					~
	200	0.05	0.17	-14.33	3.5E-8	~
	300	0.06	0.13	~		~
	500	0.10	0.14	~		~
	800	0.09	0.13	~		~
3 - 4	25	0.31	0.29	0.08	5.2E-4	1.5E-3
	50	0.32	0.31	0.03	1.5E-3	1.7E-3
	100					~
	150	0.20	0.14	39.7	6.0E-8	8.2E-5
	200	0.14	0.10	~	~	~
	300	0.13	0.11	~	~	~
	500	0.12	0.11	~	~	~
	800	0.15	0.11	~	~	~
8 to 9	25	0.27	0.28	-0.058	1.6E-4	-4.5E-4
	50	~	~			~
	100	0.25	0.17	3.75	6.5E-6	1.3E-2
	150	0.15	0.18	-16.1	9.0E-9	~
	200	~	~			~
	300	~	~			~
	500	0.13	0.10	~		~
	800	~	~			~
4 up	25	0.28		0.37	4.3E-4	6.2E-2
	50	0.30		-1.91	-3.4E-4	-2.5E-1
	100	0.25		-295.9	-8.7E-6	-9.9E-1
	150	0.14		~		~
	200	0.10		~		~
	300	0.12		~		~
	500	0.11		~		~
	800	0.11		~		~

9 up	25 50 100 150 200 300 500 800	0.29 0.30 0.17 0.19 0.16 0.14 0.13 0.10		1.24 -27.4 -1.98 -142.56 -64.6	4.9E-4 3.3E-4 4.9E-8 2.6E-8 1.0E-12	2.3E-1 -7.1E0 -7.6E-5 -2.8E-3 -1.0E-4 ~ ~ ~
NET	25 50 100 150 200 300 500 800				 Total	0.2 0.002 3.2 0.5 0.003 ~ ~ ~ 4

At this site there was evidence of a downward gradient of hydraulic potential. There was a rapidly decreasing water content between 50 and 200 cm depth. Despite the change in material properties over this part of the profile, these water content gradients nevertheless translated into hydraulic potential gradients as indicated in the above table. The soil water was evidently being generated from the short stretch of slope above the area monitored, and the flux of water was apparently directed towards the 200 cm level. Beyond this level, down to 800 cm, there was no apparent movement of water since the potential gradients were small and the hydraulic conductivities of these dry soils were extremely low.

The estimate of the net amount of soil water moving downward in the 50 to 200 cm layer and not exiting these layers (therefore being taken up by the trees) amounts to 4 litres per day per tree. This amounts to approximately 0.25 mm per day over the

representative soil volume serving the four sample trees.

4.3.8 Summary

In contrast to the two Frankfort sites, the sample trees experienced severe stress at this site. The 1994/95 rainfall was below-average, and resulted in especially acute stress developing in the sample trees towards the end of the 1995 winter. By this time, stomatal conductances were very low, LAI was considerably reduced, and pre-dawn XPP was very similar to the mid-day minimum. Despite this high degree of stress, growth did not stop, but continued at a slowed rate. It was decided to delay setting out the plastic sheeting until the soil profile had recharged from the 1994/95 summer rains. These rains resulted in a recovery of stomatal conductance, leaf area, sap flow rate, XPP and trunk growth rate. The plastic sheeting was laid out in April 1995 towards the end of the summer rains, and probably did not appreciably hasten the soil drying rate over the following winter. It is therefore likely that the trees experience regular winter-time stress due to soil water deficits, which is more accentuated after relatively poor summer rains. Tree water use in winter is effectively limited by a reduction in leaf area, as well as by reduced stomatal conductance. An interesting observation is that leaf area index declined substantially between January 1994 and January 1995, but this difference was not apparent in the daily sap flow totals. It must be concluded that the stomatal conductance of the remaining leaves increased to offset the leaf area decline. Trunk growth rates were slowed by winter stress, but did not cease at any point.

The data have demonstrated further complications to the method of predicting sub-optimal transpiration rates from soil water content. The trees at this site obviously experience some degree of regular winter stress due to insufficient soil water. They appear to have adapted through seasonal reductions in leaf area, as well as through reduced stomatal conductance. Summer-time peak leaf area development is likely to be constrained by the degree of stress developing in the previous winter. In contrast to sites 1 and 2, therefore, leaf area is constantly adjusting to seasonal (and probably even year to year) changes in soil water availability. The prediction of a potential transpiration rate is therefore complex, and any model must take leaf area into account. Even with the amount of leaf area accounted for, the stomatal conductance per unit of leaf area is undoubtedly lower than in trees growing in high rainfall sites. The potential transpiration rate found in the Frankfort trees will therefore be higher than the potential rate for the Legogote trees. There is no guarantee that this potential rate remains stable, since consecutive years of above average rainfall may lead to the development of leaves with a higher stomatal conductance.

Quantifying the rooting zone and the availability of soil water to the trees remains problematic at this site. Reductions in volumetric soil water contents were recorded throughout the top 8 m of the profile, although those recorded below 2 m appear to be very much less than were recorded at site 1. The drilling contractor reported no sign of moisture when drilling down to bedrock at 18 m. Given the relatively low rainfall at this site, it is unlikely that the profile wets up appreciably below 8 m, implying that trees are unlikely to obtain a substantial proportion of their water

requirement from below 8 m.

The analysis of hydraulic potential gradients revealed a downward gradient of hydraulic potential between 50 and 200 cm. This flux of water originated from the area immediately up slope of the experimental site. There was no apparent vertical movement of water between 200 and 800 cm, confirming the pattern of neutron probe readings (figure 31). The lack of deep reserves of water at this site clearly contributed to the development of severe stress in the trees. The estimated net influx amounted to approximately 0.25 mm per day, which, when added to the apparent soil water uptake of 0.41 mm per day, would bring the total water availability of the profile to 0.66 mm per day, closer to the tree water use rate of 0.86 mm per day. The trees were clearly surviving on soil water within the top 200 cm of the surface. The absence of soil water reserves below 200 cm is intriguing. The relatively low rainfall and high evaporative demand at this site are likely to reduce the chance of deep penetration of rainfall.

5. DISCUSSION AND CONCLUSIONS

The experiments have clearly shown that the method of soil water accounting to link soil water content to the fraction of potential transpiration taking place is impractical in plantations of *E. grandis*. This conclusion is based on the following findings:

- Extremely deep permeable profiles and root systems. Several published reports of Australian *Eucalyptus* trees rooting to depths of 18 m (Carbon *et al.*, 1980), 28 m (Nulsen *et al.*, 1986) and 15 m (Kimber, 1972) support the observations from this study. Deep drilling at site 1 has revealed live tree roots at 28 m below the surface, illustrating the impracticality of modelling soil water changes throughout the entire rooting zone.

- Unknown volume of stones, especially in deeper horizons. The sites chosen for this study were characterized by stone-free soils in the first 8 m of the profiles. A high proportion of forestry soils will have appreciable quantities of stones, complicating soil water balance modelling. A high degree of variation in depth to bedrock and the water content of deep subsoil has been shown. High spatial variability in stone volume must be expected on most sites.

- A recent soil water study in an *E. grandis* compartment on Kruisfontein estate has shown clear evidence of substantial lateral flow of soil water down slope along an eluvial soil horizon. This phenomenon could be more widespread, introducing formidable complexity to any soil water balance modelling.

- Physiological adaptions of trees experiencing regular seasonal soil water deficits. Comparison of sap flows, leaf area index and stomatal conductance between the Frankfort sites and the Legogote site led to the realization that potential transpiration models developed from trees in sites with high rainfall and deep soils will overestimate water use of trees in such drier sites, even during the summer months when soil water availability is high. I hypothesize that the site 3 trees experience regular stress during each winter, and that this leads to adaptions involving lower stomatal conductances, lower sapwood moisture content and lower leaf area indices, which reduce the water use of the trees. A comparison of the relation between daily sap flow and the mean daily VPD for a sample of summer-time days at all three sites (figure 36) shows the different rates of water use. None of the trees experienced stress during these periods. From a comparison of sites 1 and 3 (where tree density was similar), it can be deduced that differences in leaf area were largely (although not wholly) responsible for the differences in sap flow. LAI at site 1 was very close to 3, whereas at site 3 it was increasing above 1.5 over the sample period. Figure 36 shows that daily water use at site 3 was somewhat less than half of site 1, suggesting that reduced stomatal conductance also plays a role in limiting the water use of the trees at this site. The significance of these adaptions is that one cannot assume the same potential rate of transpiration in all well-watered trees, even if differences in leaf area are taken into account.

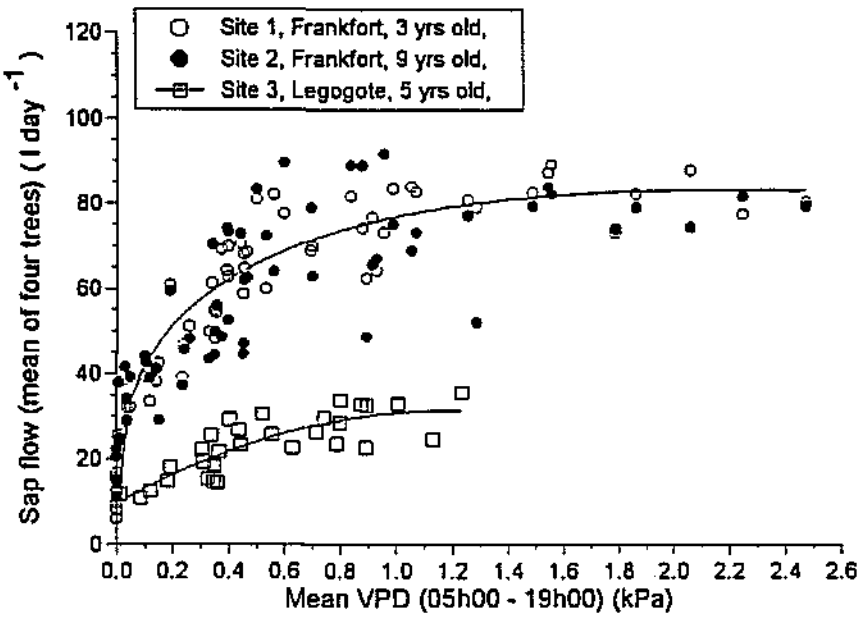

Figure 36. The relation between mean daily VPD (05h00 - 19h00) and total daily sap flow (mean of four trees) at sites 1, 2 and 3. Data from sites 1 and 2 were recorded in November and December 1992, while the site 3 data were recorded in January and February 1995.

- An additional looming problem to the feasibility of the soil water balance method is the increasingly widespread use of clones (often hybrids) by eucalypt growers, which are known to have significantly different growth and water use characteristics. The relation between transpiration rate and soil water content would regularly have to be described for each newly introduced

The authors opinion is that the only alternative approach to estimating the water use of *E. grandis* plantations over a wide range of sites is to use the growth rates of the

trees themselves as indicators of site conditions and water use. This presupposes that there is a useful correlation between growth and water use. It can be reasoned that trees which experience a greater degree of moisture stress will also grow more slowly due to stomatal closure and reduced leaf area index. Thus, differences in growth increments within catchments are likely to reflect differences in duration and intensity of soil water deficits, and hence annual water use.

The early results from the Frankfort sites prompted the initiation of a separate study of the growth and water use of *E. grandis* trees showing a very wide range of vigour within a heterogeneous catchment on Kruisfontein estate in the vicinity of White River, Mpumalanga. The aim was to determine the degree of correlation between annual volume growth increment in the trunks and the total water use over the same period, to ascertain if growth could be used to infer water use. The study lasted a full 12 months since it was realized that seasonal patterns of water use and growth are different, leading to seasonal variation in water use efficiency. The high degree of correlation in the 17 sample trees is evident in figure 37. The growth and water use data from sites 1 and 3 (where 12 months of data are available) conform to the trend, and suggest that the correlation is relatively stable for the genotypes used and conditions experienced at the different sites. The exciting implication of this correlation is that maps of year-to-year volume growth increments can be obtained for even the most heterogeneous catchments and used to estimate the annual water use of the trees. This could lead to vastly improved understanding of the impacts of *E. grandis* on our water supplies, and recognition of gains in water use efficiency which may be achieved in newly developed clones.

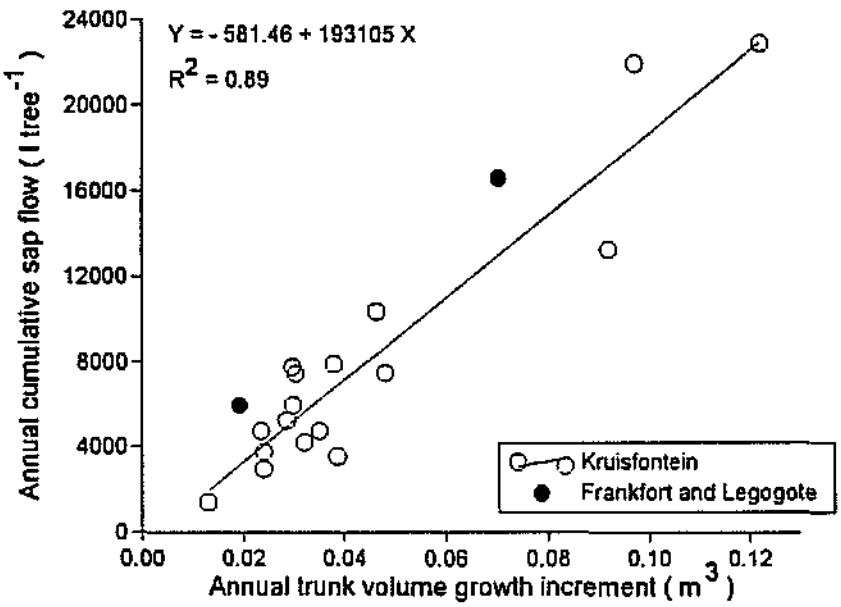

Figure 37. The relation between yearly volume growth increment and yearly total sap flow recorded in 17 sample trees in a separate study at Kruisfontein. The mean volume growth and total sap flow recorded at sites 1 and 3 are also shown.

6. RECOMMENDATIONS FOR FURTHER RESEARCH

- Further investigation of the relation between annual volume growth increment and annual water use for a representative range of tree ages, site qualities, climates, genotypes and plantation management regimes. Further perspective on this relationship is required before it can be used for practical purposes. Appropriate studies are already underway.

- The reliance of the Frankfort trees on soil water stored at depths beyond 8 m raises questions about how such deep soil water reserves can be replenished, especially under continuous *Eucalyptus* cropping. If abstraction is greater than recharge in the long term, then the trees will suffer increasing soil water deficits and reduced growth rates. Such declines in yields have been reported to be numerous (Boden, 1990). Greater understanding of the long-term water balance of eucalypt plantations at such sites is required to assess the sustainability of continuous eucalypt cropping, and evaluate what management practices can be adopted to minimize growth losses. The intensive soil analyses performed in this study have demonstrated that significant vertical fluxes of soil water take place in response to gradients in water potential. This phenomenon needs to be taken into account in future studies of soil water dynamics in deep forest soils.

  The influence of eucalypts in depleting such deep soil water reservoirs and causing significant lags in the response of streamflow to afforestation or

deforestation also requires further study. Data from the Mokobulaan research catchments in Mpumalanga has demonstrated the existence of extremely deep (30-45 m) permeable, moist profiles (Dye and Poulter, 1991) which are potentially accessible to deep rooted *Eucalyptus* trees. A five-year lag in streamflow recovery following clearfelling of a catchment planted to *E. grandis* was recorded (Scott and Lesch, 1996), suggesting that abstraction of soil water in deep soil/subsoil profiles may cause significant lags in streamflow response to management activities within the catchment.

- This study has produced a wealth of data which should prove useful in validating and refining existing forest hydrological models.

7. LIST OF PAPERS AND ARTICLES PUBLISHED

Dye, P.J. 1993. The reaction of *Eucalyptus grandis* to induced drought. In: Proceedings of the Sixth South African National Hydrological Symposium, Pietermaritzburg, 8-10 September 1993. pp 725-735.

Dye, P.J. 1994 Differences in soil-water use by Eucalypts and Pines. FORESTEK, 3, no. 2, winter 1994: 3-4.

Dye, P.J., Soko, S. and Maphanga, D. 1994. An investigation of the patterns of soil water uptake under stands of *Pinus patula* and *Eucalyptus grandis*. CSIR report FOR-DEA 743.

Dye, P.J., Olbrich, B.W. and Everson, C.S. 1995. The water use of plantation forests and montane grassland in summer-rainfall forestry regions of South Africa. In: Proceedings of the Seventh South African National Hydrological Symposium, Grahamstown, 4-6 September, 1995.

Dye, P.J. 1996a. Response of *Eucalyptus grandis* trees to soil water deficits. Tree Physiology 16: 233-238.

Dye, P.J. 1996b. Climate, forest and streamflow relationships in South African afforested catchments. Commonwealth Forestry Review, 75: 31-38.

8. ACKNOWLEDGEMENTS

The research in this report emanated from a project funded by the Water Research Commission and entitled:

"The determination of the relationship between transpiration rate and declining available water for Eucalyptus grandis"

The Steering Committee responsible for this project consisted of the following persons:

Dr G. Green	Water Research Commission (Chairman)
Mr D. Huyser	Water Research Commission (Secretary)
Mr H. Maaren	Water Research Commission
Dr P. Reid	Water Research Commission
Mr N. Lecler	University of Natal
Mr B. Metelerkamp	ICFR
Mr J. Musto	ICFR
Professor M. Savage	University of Natal
Professor R. Schulze	University of Natal
Dr D. Van der Zel	Department of Water Affairs and Forestry
Mr D. Versfeld	CSIR

The financing of the project by the Water Research Commission and the

contribution of the members of the Steering Committee is gratefully acknowledged.

SAFCOL and HL&H are thanked for permission to conduct the experiments on Frankfort and Legogote plantations. Dr Simon Lorentz and his team are acknowledged for their thorough soils investigation which contributed much to this study.

9. REFERENCES

Ankeny, M.D. 1992. Methods and theory for unconfined infiltration measurements. *In:* Topp, G.C., Reynolds, W.D. and Green, R.E. (eds). Advances in measurement of soil physical properties: bringing theory to practice. Soil Science Society of America Special Publication, 30:123-142, Madison, WI.

Boden, D.I. 1990. The relationship between soil water status, rainfall and the growth of *Eucalyptus grandis.* Paper presented at the 19th IUFRO World Congress, August 1990, Montreal, Canada. 12 pp.

Calder, I.R. 1992. A model of transpiration and growth of *Eucalyptus* plantation in water-limited conditions. Journal of Hydrology. 130: 1-15.

Carbon, B.A., Bartle, G.A., Murray, A.M. and McPherson, D.K. 1980. The distribution of root length, and the limits to flow of soil water to roots in a dry sclerophyll forest. Forest Science, 26: 656-664.

Coetzee, J. 1992. A revised tree volume table for short rotation *Eucalyptus grandis* timber crops. ICFR Bulletin 9/92, Pietermaritzburg. 5 pp.

Couchat, P., Carre, C., Marcesse, J. And Le Ho, J. 1995. Application to the calibration of neutron moisture gauges and to the pedological study of the soil. Proceedings of a Conference on Nuclear Cross Sections in Technology,

Washington DC, March 1995.

Dunlap, F. 1912. The specific heat of wood. USDA Forest Service Bulletin No. 110. 28 pp.

Dunnin, F.X.and Aston, A.R. 1984. The development and proving of models of large scale evapotranspiration: an Australian study. Agricultural Water Management. 8: 305-323.

Dye, P.J. 1993. Development of generalized models of rainfall interception by *Eucalyptus grandis* and *Pinus patula* plantations. CSIR report FOR-DEA 623.

Dye, P.J. and B.W. Olbrich. 1991. A transpiration model applicable to six-year-old *Eucalyptus grandis* trees growing under conditions of sufficient soil water availability. CSIR internal report.

Dye, P.J. and Poulter, A.G. 1991. An investigation of sub-soil water penetration in the Mokobulaan research catchments, South-Eastern Transvaal. South African Forestry Journal, 161: 31-34.

Food and Agricultural Organization of the United Nations (FAO). 1974. Legend to the Soil Map of the World. UNESCO, Paris.

Greacen, E.L. 1981. Soil water assessment by the neutron method. CSIRO,

Australia.

Huber, B. and Schmidt, E. 1937. Eine kommpensationsmethode zur thermoelektrischen messung langsamer saftstrome. Die Berliner Deutsche Botanische Geselschaft. 55: 514-529.

Hutson, J.L. 1984. Estimation of hydrological properties of South African soils. University of Natal, Pietermaritzburg, Department of Soil Science and Agrometeorology. Unpublished Ph.D. dissertation, 232 pp.

Kimber, P.C. 1972. The root system of Jarrah (*Eucalyptus marginata*). Western Australian Forestry Department, Research paper No. 10.

Lorentz, S.A. 1993. The use of accurate liquid retention characteristics of porous media in hydrology. *in*: Lorentz S., Kienzle S., and Dent M. *eds.* Proceedings of the Sixth South African Hydrological Symposium 8-10 September. Univ. of Natal, Pietermaritzburg.

Lorentz, S.A. 1994. Measurement of retention and hydraulic conductivity characteristics of porous media using a modified controlled outflow cell. ASA-CSSA-SSSA 1994 Agronomy Abstracts.

Lorentz, S.A., Ballim, F. and Pretorius, J.J. 1996. Estimation of soil water flux in Frankfort and Legogote forest soils, Sabie. ACRUcons Report 10.

Department of Agricultural Engineering, University of Natal, Pietermaritzburg.

Lorentz, S.A., Durnford, D.S. and Corey, A.T., 1991. A controlled outflow method of measuring liquid retention in porous media. ASA-CSSA-SSSA 1991 Agronomy Abstracts.

Louw, J.H. 1993. A forestry land system classification of region F. CSIR report FOR-DEA 614, Pretoria.

Marshall, D.C. 1958. Measurement of sap flow in conifers by heat transport. Plant Physiology, 33: 385-396.

Nulson, R.A., Bligh, K.J., Baxter, I.N., Solin, E.J. and Imrie, D.H. 1986. The fate of rainfall in a mallee and heath vegetated catchment in southern Western Australia. Australian Journal of Ecology, 11: 361-371.

Olbrich, B.W. 1991. Verification of the heat pulse velocity technique for estimating sap flow in *Eucalyptus grandis*. Canadian Journal of Forest Research, 21: 836-841.

Olbrich, B.W. 1994. The application of the heat pulse velocity technique to the study of transpiration from *Eucalyptus grandis*. Unpublished Ph.D. thesis, University of Natal, Durban, South Africa.

Pearcy, R.W., Ehleringer, J., Mooney, H.A. and Rundel, P.W. 1989. Plant Physiological Ecology. Chapman and Hall, London.

Ritchie, G.A. and Hinckley, T.M. 1975. The pressure chamber as an instrument for ecological research. Advances in Ecological Research, 9: 165-254.

Scott, D.F. and Lesch, W. 1996. Streamflow responses to afforestation with *Eucalyptus grandis* and *Pinus patula* and to felling in the Mokobulaan experimental catchments, Mpumalanga Province, South Africa. (In prep).

Swanson, R.H. 1974. A thermal flowmeter for estimating the rate of xylem sap ascent in trees. In: Flow - Its measurement and Control in Science and Industry (Ed. R.B. Dowdell), pp 647-652. Instrument Society of America, Pittsburgh.

Swanson, R.H. and D.W.A. Whitfield. 1981. A numerical analysis of heat pulse velocity theory and practice. Journal of Experimental Botany, 32: 221-239.

Vachaud, G., Royer, J.M. and Cooper, J.D. (1977). Comparison of methods of calibration of a neutron probe by gravimetry or neutron capture model. Journal of Hydrology, 34: 343-356.

Van Zijl, J.S.V. (1985) A practical manual on the resistivity method. CSIR Report K79, 136 pp.